Unveiling a missing component of the atypical type IV secretion system required for natural transformation of *Helicobacter pylori*

J. Francisco Villa[1], Sumedha Kondekar[1], Yoann Fauconnet[2], Mérick Machouri[1], Céline Lacrouts[1], Xavier Veaute[3], Raphaël Guérois[2], Eduardo P. C. Rocha[4], Jessica Andreani[2]* and J. Pablo Radicella[1]*

[1] Université Paris-Saclay, Université Paris Cité, CEA, Stabilité Génétique Cellules Souches et Radiations, DRCM, Institut de Biologie François Jacob, F-92260 Fontenay aux Roses, France
[2] Université Paris-Saclay, CEA, CNRS, Institute for Integrative Biology of the Cell (I2BC), F-91198 Gif-sur-Yvette, France
[3] Université Paris-Saclay, Université Paris Cité, CEA, INSERM, Stabilité Génétique Cellules Souches et Radiations, DRCM, Institut de Biologie François Jacob, F-92260 Fontenay aux Roses, France
[4] Institut Pasteur, Université de Paris Cité, CNRS UMR3525, Microbial Evolutionary Genomics, Paris, France

*Corresponding authors

pablo.radicella@cea.fr (JPR) ; jessica.andreani@i2bc.paris-saclay.fr (JA)

Abstract

Exchange of genetic information by natural transformation shapes bacterial evolution. In *Helicobacter pylori* it is thought to drive its unusually high recombination rate, which has a crucial role in the evolution of virulence and the propagation of antibiotics resistance genes. While in most cases uptake of the incoming DNA into the periplasm is mediated by type IV pili, in *H. pylori* this initial step of natural transformation requires ComB, a unique competence-specific type IV secretion system (T4SS). The mechanisms by which ComB mediates DNA uptake are still poorly understood, since T4SS are usually involved in an opposite process of DNA export. Here, we identify a gene (*hp1421*) that is absolutely required for uptake of the transforming DNA into the periplasm, although distant from the *comB* operons. We show that *hp1421* codes for a hexameric ATPase from the VirB11 family. HP1421 is present in the cytoplasm and interacts with ComB4, another ATPase of the T4SS inner membrane subcomplex. The structural modelling and functional analysis of HP1421 and its interaction with ComB4 indicate that HP1421 is a missing component of the ComB inner-membrane subcomplex that we propose to name ComB11. Phylogenetic analyses show that *comB11* is a *H. pylori* core gene and suggest that the competence-dedicated ComB T4SS was a recent acquisition within *Helicobacteraceae.* Hence, co-option of the T4SS for DNA transformation requires nearly all the proteins that were previously essential for DNA conjugation.

Author Summary

The capacity of bacteria to exchange genetic information contributes in the case of pathogens to the spreading of antibiotic resistance and virulence factors. For *Helicobacter pylori,* a Gram-negative pathogen that colonises about half of the world population and is at the origin of diseases such as ulcers and gastric cancers, natural transformation is the major mechanism of horizontal gene transfer. However, *H. pylori* uses a very unusual system to capture and internalise the foreign DNA. Indeed, a Type 4 secretion system mediates this process. Here, we identify a so far missing and essential component of the T4SS, coded by a gene distant from the operon coding the other subunits. Through a combination of structural modelling, biochemical and microscopy approaches we show that this ATPase is an

54 indispensable part of the ComB T4SS. Our study provides new insights into the mechanism
55 by which the peculiar ComB T4SS works backwards to allow the passage of the tDNA from
56 the bacterial environment into the periplasm.

Introduction

Horizontal gene transfer strongly contributes to the adaptive potential of bacterial populations by accelerating evolutionary rates through the spread of non-selected genetic variants[1–4]. In pathogens, virulence and antibiotic resistance are often associated with horizontal gene transfer. This has been well documented in the case of *Helicobacter pylori,* where high spontaneous mutation rates combined with extensive horizontal gene transfer underlie the amazing genome plasticity of the species that contributes to its success as a pathogen [5,6].

Natural transformation (NT) is one of the three main pathways of horizontal gene transfer. During NT, free DNA present in the environment is captured and integrated into the bacterial genome. This mechanism is considered to be the main pathway for horizontal genetic exchange in *H. pylori[7]* and to play a crucial role in the pathogen persistence in the host and chronicity due to adaptation and immune response evasion[8,9]. Unlike other horizontal gene transfer pathways, NT only relies on molecular machineries coded by the recipient cell[10,11]. The initial event in NT consists in the capture of the exogenous DNA on the cell surface. It is then transferred into the cytoplasm through a two-step mechanism[12,13]. In naturally competent bacteria, uptake of the transforming DNA (tDNA) from the bacterial surface into the periplasm, through either the cell wall in gram-positive bacteria or the outer membrane in gram-negative, requires type IV pili or pilus-like structures. The tDNA is then bound by ComEA (ComH in *H. pylori*) and delivered, as a single-stranded DNA, to the inner membrane protein ComEC that, together with the cytosolic ComFC[14], mediates its transport into the cytosol. Remarkably, uptake to the periplasm in *H. pylori* is mediated by a unique set of type IV secretion system (T4SS) proteins rather than by type IV pili[15,16]. T4SS originated as a system for DNA exchange by conjugation in diderm bacteria to give rise to a variety of protein secretion systems present in both monoderm and diderm bacterial species[17]. One of the most surprising adaptations of T4SS to new functions is the ComB system from *H. pylori[18]*, required for NT. Indeed, ComB is the only T4SS studied so far that, instead of mediating a secretion process, mediates the internalisation of a macromolecule. Components of this simplified T4SS are coded by two independent operons, *comB2-comB4* and *comB6-comB10,* named after the homologous proteins in the well characterised VirB/D4

89 T4SS from *Agrobacterium tumefaciens[19].* However, when compared to the *A. tumefaciens*
90 minimized system, some ComB components seem to be missing[20]. B1, involved in murein
91 hydrolysis, might be replaced by the ComL homologue, required for NT in *Neisseria*
92 *gonorrhoeae.* B1 could also be dispensable for the process since it is not essential for DNA
93 export. In addition to B1, the *comB* operons do not code for VirB5, VirD4 or VirB11
94 homologues. While the absence of VirB5, a minor pilin, and VirD4, a traffic ATPase involved
95 in substrate recruitment, could be expected in a T4SS mediating the internalisation of DNA
96 rather than the secretion of macromolecules, that of a VirB11 homologue is surprising. VirB4
97 and VirB11 are ATPases localised at the cytoplasmic face of the inner membrane[21]. In the
98 studied T4SS systems, these so-called secretion ATPases are essential for T4SS functions.
99 Here we identified and characterised a gene coding for a VirB11 homologue essential for NT.
100 The resulting protein is a *bona fide* ATPase, transiently associated with the bacterial
101 membrane. Its interaction with ComB4 is indispensable for the entry of the tDNA into the
102 periplasm. We propose therefore to name it ComB11.
103
104 **Results**
105
106 **HP1421 is required for natural transformation**. A homology search for VirB11-type ATPases
107 pointed, in addition to the Cag-associated and well characterised HP0525 (Cagα), to the
108 protein coded by *hp1421.* Sequence alignment of the two *H. pylori* genes with *A.*
109 *tumefaciens* VirB11 show a high degree of homology and, in particular, a strong conservation
110 of residues essential for the VirB11 and HP0525 ATPase activities (S1 Fig.). While HP1421 has
111 been proposed to be a VirB11 homologue for the ComB system[20], a transposon insertion in
112 codon 20 of *hp1421* did not result in a defect in plasmid transformation[22]. Since that
113 mutant preserved most of the open reading frame (ORF), including the region harbouring
114 the putative active sites, production of an active protein could not be ruled out.
115 Furthermore, transformation with genomic DNA was not tested on that strain. We thus
116 decided to create a null mutant by replacing the whole *hp1421* ORF by a non-polar antibiotic
117 resistance cassette and test its capacity to be transformed by genomic DNA of a streptomycin
118 resistant (Strep^R) but otherwise isogenic strain.
119 Fig. 1A shows that inactivation of *hp1421* resulted in transformation levels below the
120 detection limit of the assay, which is defined by the frequency of spontaneous Strep^R
121 mutations. In order to rule out polar effects caused by the insertion of the cassette, we

122 reintroduced in non-essential loci constructs expressing the *hp1421* ORF with a FLAG tag
123 coding sequence fused 5' of it. In the first case, the gene was under the control of the strong
124 *ureA* promoter, while in the other, introduced into the *rdx* locus, the weaker *comH* promoter
125 was used. In both cases, the NT capacity was completely restored to wild type levels,
126 confirming the essential role of HP1421 in NT.
127
128 **Figure 1. HP1421 is essential for natural transformation**. **A)** Natural transformation frequencies for
129 indicated *H. pylori* strains. Data represent Mean + SEM (n=7→17). Different lowercase letters indicate
130 significant differences ($p<0.05$) between treatments (SNK test). The horizontal line at $1.99x10^{-7}$ indicates
131 frequencies of revertant due to spontaneous mutations in absence of donor DNA in the wild type strain.
132 **B)** Transformation frequencies after electroporation with streptomycin resistance genomic DNA donor.
133 Data represent Mean + SEM (n=4). Different lowercase letters indicate significant differences ($p<0.05$)
134 between treatments (Tukey's Test).
135
136 **HP1421 participates in the initial steps of NT.** The NT process can be divided in four distinct
137 steps[10]: capture of the tDNA at the surface of the cell, its uptake into the periplasm, its
138 transport through the inner membrane and finally its integration into the bacterial genome
139 by homologous recombination. To establish where in this process HP1421 acts, we first
140 tested the capacity of the *Δhp1421* strain to be transformed by electroporation. As shown in
141 Fig. 1B, introducing the tDNA by this method resulted in transformation frequencies of the
142 *Δhp1421* strain equivalent to those of the *wild type*, indicating that HP1421 is required at
143 some point upstream of the recombination step, in agreement with the hypothesis of a role
144 linked to the ComB system.
145 To confirm that HP1421 is required for the tDNA entry to the cell, we used the whole-
146 cell duplex PCR-based DNA uptake assay that allows the detection of heterologous tDNA
147 presence either in the periplasm or in the cytoplasm [14,23,24]. The assay showed that the
148 tDNA cannot be detected inside the *Δhp1421* cells but the signal was recovered after
149 complementation of the knockout strain with HP1421 expressed from the *ureA* locus (Fig.
150 2A,B).
151
152 **Figure 2. HP1421 is involved in capture and/or uptake of transforming DNA**. **A)** Internalized donor DNA
153 was monitored by PCR. Amplification products were visualized by 1% agarose gel electrophoresis. **B)**
154 Percentage ratios of donor versus recipient amplification, results were normalized with respect to

155 the wild-type strain. Data represent Mean + SEM (n=3). Different lowercase letters indicate significant
156 differences (p<0.05) between treatments (Tukey's Test). **C)** Fluorescent cy3-λDNA foci formation in *H.*
157 *pylori wild-type, ΔcomB2 Δhp1421 and Δhp1421 ureA::FLAG-hp1421* strains. Z maximum projections of
158 merged images of Cy 3.5 (red channel) and bright field are presented. **D)** Percentage of bacteria with
159 fluorescent DNA foci. Data represent Mean + SEM (n=4→8). Different lowercase letters indicate significant
160 differences (p<0.05) between treatments (Tukey's Test).
161
162 Canonical T4SS systems provide a direct passage between the cytosol and the
163 extracellular compartment. During NT, the delivery of the tDNA from the surface of the cell
164 to the cytoplasm is a two-step mechanism[12,13]. In *H. pylori*, the uptake across the outer
165 membrane is mediated by ComB while the passage through the inner membrane depends on
166 the conserved ComEC protein[25,26]. If HP1421 is a VirB11 homologue associated with
167 ComB, we expected HP1421 to be implicated in the first of those steps. To validate this
168 hypothesis, we monitored the accumulation of tDNA in the periplasm using a fluorescently
169 labelled tDNA. Previous work had shown that fluorescent tDNA foci are detected and
170 stabilised in *H. pylori comEC* mutants[26,27]. In the absence of HP1421, periplasmic foci were
171 undetectable, as in a *ΔcomB2* mutant (Fig. 2C,D). Again, complementation by expression of
172 the *wild-type* HP1421 protein resulted in the recovery of the foci. Taken together, these
173 results implicate HP1421 in the initial step of NT leading to the delivery of the tDNA into the
174 periplasmic space.
175
176 **HP1421 is a cytoplasmic ATPase.** Sequence homology with ATPases of the VirB11 family (S1
177 Fig.) strongly suggests that HP1421 has an ATPase activity. To confirm this, we expressed in
178 *Escherichia coli* the HP1421 protein fused through its N-terminal end to a maltose binding
179 protein (MBP) tagged with six histidine residues (6-His-MBP-HP1421, herein MBP-HP1421).
180 The fusion protein was purified (S2A Fig.) but attempts to obtain HP1421 without the MBP
181 were unsuccessful, the protein precipitating after cleavage of the MBP. The ATPase activity
182 was measured by determining the release of phosphate as a function of the substrate (ATP)
183 concentration (Fig. 3A). MBP-HP1421 displayed a strong ATPase activity, with a calculated K_m
184 of 29.8 μM ATP, a value in agreement with those obtained for other enzymes of the VirB11
185 family[28,29]. In parallel, equivalent constructs were used to express Walker A motif mutants
186 of the protein (E176A and E176K). Neither of those variants showed ATPase activity (Fig. 3A
187 and S6A Fig.). Since the purification protocol was identical to the one used for the wild-type

188 protein, these results rule out the presence of contaminating activities and confirm that
189 HP1421 is a *bona fide* ATPase.
190
191 **Figure 3**. **HP1421 is a cytoplasmic hexameric ATPase**. **A)** ATPase activity of purified HP1421 versions as a
192 function of ATP concentration, Pi released during ATPase enzymatic reactions was followed by
193 spectrometry. **B)** BACTH analysis to assess the interaction between the indicated alleles of HP1421. **C)**
194 Chromatogram for size exclusion chromatography (SEC) of 6xHis-MBP-HP1421 using a Superdex 200
195 column **D)** AlphaFold3 prediction made using 6 copies of HP1421 and 6 ATP molecules (pTM = 0.77, ipTM
196 = 0.75, and chain-pair ipTM = 0.73 between any two monomers of HP1421 interacting in the model). One
197 copy of HP1421 is highlighted from the model for visualization purpose. **E)** Western blot of subcelular
198 fractions for indicated *H. pylori* strains.
199
200 As it is the case with most ATPases, HP1421 is expected to form multimers. To test
201 whether the HP1421 monomers interact between themselves, a bacterial adenylate-cyclase
202 two hybrid (BACTH) assay was carried out. This analysis revealed that indeed HP1421 form at
203 least dimers (Fig. 3B). To establish the degree of multimerization, gel filtration assays on the
204 purified MBP-HP1421 were performed with a Superdex 200 column. The main peak
205 containing the fusion protein eluted at a volume corresponding to a molecular weight of
206 approximately 460kDa which is close to that of an MBP-HP1421 hexamer, 473kDa (Fig. 3C,
207 S2B Fig.). This is in agreement with a structural model of a HP1421 hexamer predicted by
208 AlphaFold3[30] with a high level of confidence (Fig. 3D). This predicted HP1421 hexamer is
209 structurally very similar to the experimental structure of the HP0525 hexamer (PDB
210 identifier: 6BGE, S3A Fig.). Additionally, including 6 ATP molecules in the AlphaFold3 model
211 of the HP1421 showed that ATP was confidently predicted as bound into a pocket on the
212 surface of the HP1421 hexamer and in contact with residue E176 in the model (S3B Fig.).
213 T4SS-associated VirB11-like ATPases were reported to be localised in both, soluble
214 and membrane fractions[31–33]. To examine HP1421 distribution within the cell, the soluble
215 and membrane fractions from a *H. pylori* strain expressing the active FLAG tagged protein
216 (Fig. 1A) were separated. Western blot analysis showed that while the majority of HP1421 is
217 present in the soluble extract, a fraction of the protein can be detected associated with the
218 membranes (Fig. 3E). When we analysed the localisation of HP1421 E176K, the balance
219 between the two fractions was inverted, the majority of the mutant protein being associated
220 with the membranes. Interestingly, in *Legionella pneumophila* Dot/Icm T4SS, DotB, the

221 VirB11 homologue, is found essentially in the cytoplasm with only in a fraction of bacteria
222 displaying DotB foci at the cellular pole. However, the E191K mutant, equivalent to HP1421
223 E176K and previously shown to bind but not hydrolyse ATP[34], was almost exclusively found
224 at the bacterial pole[35].
225 The active site mutants provide a tool to determine if HP1421 ATPase activity is
226 needed for its function in NT. We thus tested complementing the *⊿hp1421* strain phenotypes
227 with either HP1421 E176K or HP1421 E176A expressed from the *ureA* promoter. Unlike that
228 of the wild-type protein (Fig. 1A), the expression of the active site mutants did not allow the
229 recovery of the transformation capacity (Fig. 4A) nor the accumulation of fluorescently
230 labelled tDNA in the periplasm (Fig. 4B). Together, these results show that HP1421 is an
231 hexameric ATPase whose enzymatic activity is indispensable for NT.
232
233 **Figure 4. HP1421 ATPase activity is crucial to for NT**. **A)** Natural transformation frequencies for indicated
234 *H. pylori* strains. Data represent Mean + SEM (n=4→5), the horizontal line 1.99X10-7 indicates frequencies
235 of revertant due to spontaneous mutations in absence of donor DNA in the wild type strain. **B)**
236 Fluorescent cy3-λDNA foci formation in *H. pylori strains*. Z maximum projections of merged images of Cy
237 3.5 (red channel) and bright field are presented.
238
239 **HP1421 interaction with ComB4 is critical for NT.** Structural and biochemical approaches
240 revealed an interaction between VirB11 orthologues and their cognate VirB4 in various T4SS
241 models[36–38]. In silico modelling of the *H. pylori* proteins predicted with good confidence
242 that such an interaction could also occur for the HP1421-ComB4 pair. We performed
243 AlphaFold3 modeling of the interaction between a HP1421 hexamer and a ComB4 C-terminal
244 domain hexamer, yielding a very confident structural model (ipTM =0.81, pTM = 0.82, Fig. 5
245 and S4A Fig.). This model is highly structurally similar to models of the HP1421-ComB4
246 interface using single copies of the full-length proteins, obtained with high confidence by
247 AlphaFold2[39,40]and AlphaFold3 (ipTM = 0.67 with AlphaFold2, 0.66 with AlphaFold3 and
248 pTM = 0.78 with AlphaFold2, 0.75 with AlphaFold3) and to an AlphaFold2 model using only
249 the N-terminal domain of HP1421 and the C-terminal domain of ComB4 (ipTM = 0.88, pTM =
250 0.89, S4B Fig.). The HP1421 ATPase activity is mediated by the C-terminal domain and the
251 model hints that this activity should not be affected by the binding of HP1421 to ComB4. In

252 addition, the HP1421-ComB4 modeled interface is perfectly compatible with the formation
253 of a full-length ComB4 hexamer (S5 Fig).
254
255 **Figure 5. HP1421 and ComB4 double hexamer complex and interface. A)** HP1421 full length (blue) and
256 ComB4 C-terminal domain (salmon) hexamers confidently predicted as interacting with AlphaFold3 (pTM =
257 0.82, ipTM = 0.81). One copy of each protein was highlighted for visualisation purposes. **B)** Zoom on the
258 interface of the AlphaFold3 heterodimeric model highlight important residues (R8 and R60 on HP1421,
259 E548 and D559 on ComB4).
260
261 In order to empirically probe the interaction, a split luciferase assay was carried out
262 with *H. pylori* strain expressing codon-optimized long (lgbit) and small (smbit) nanoluciferase
263 fragments (S7 Fig.) fused to the N-terminal end of HP1421 and the C-terminal end of ComB4,
264 respectively. Proximity between lgbit-HP1421 and ComB4-smbit would reconstitute the
265 luciferase and produce a luminescent signal. This was indeed the case, strongly suggesting
266 that HP1421 and ComB4 interact in the cellular context (Fig. 6A). The model presented in Fig.
267 5 displayed a strong electrostatic complementary of the interaction interfaces (S8 Fig.). We
268 hypothesized that switching charges in some key interface residues could abolish the
269 interaction and thus validate the model and provide a tool to assess the biological role of the
270 interaction. Two amino-acid changes were chosen for each of the proteins based on the
271 structural model of the HP1421-ComB4 interface (Fig. 5). For HP1421, arginine 8 and 60 were
272 substituted by aspartic acid and glutamic acid, respectively. For ComB4, glutamic acid 548
273 and aspartic acid 559 were replaced by arginine. The substitutions were introduced in the
274 split luciferase constructs and the assays were carried out. As shown on Fig. 6A, substituting
275 either the arginine on the N-terminal domain of HP1421 with acidic amino-acids or the acidic
276 amino-acids in the C-terminal domain of ComB4 with arginine abolished the luminescent
277 signal, indicating a disruption of the interaction.
278
279 **Figure 6. HP1421-ComB4A interaction is necessary to allow NT**. **A)** Split-luciferase assay of interaction
280 between ComB4::SmBit and LgBit::HP1421 variants, data represent Mean + SEM (n=5→8). Different
281 lowercase letters indicate significant differences ($p<0.05$) between treatements (Tukey's test). **B)** Natural
282 transformation frequencies for indicated *H. pylori* strains. Data represent Mean + SEM (n=3→6). Different
283 lowercase letters indicate significant differences ($p<0.05$) between treatments (SNK test). The horizontal
284 line $1.99X10^{-7}$ indicates frequencies of revertant due to spontaneous mutations in absence of donor DNA

285 in the wild type strain. **C)** Western blot of total fractions for indicated *H. pylori* strains. **D)** Western-blot of
286 subcelular fractions for indicated *H. pylori* strains.
287
288 We then tested those interaction mutants for their capacity to sustain NT. For that
289 purpose, we constructed *H. pylori* strains that expressed either both wild-type genes or one
290 or the other interaction mutants. A strain expressing the HP1421 R8D-R60E variant was
291 completely impaired for transformation (Fig. 6B,C). The same result was obtained with the
292 ComB4 E548R-D559R variant (Fig. 6B,C). To rule out an effect of the amino-acid substitutions
293 on the biochemical functions of HP1421, we expressed in *E. coli* and purified MBP-HP1421
294 R8D-R60E to assess its enzymatic activity and its capacity to assemble as hexamers, two
295 properties required for its function in other T4SS[41]. As shown in S6A Fig., HP1421 R8D-
296 R60E was able to hydrolyse ATP with the same specific activity than that of the wild-type
297 protein. When the purified mutant was subjected to a gel filtration assay to determine its
298 oligomerization status, the elution profile obtained indicated the presence of an
299 approximately 460 KDa complex corresponding to a hexamer, as it was found for the wild-
300 type protein MBP-HP1421 (S6B Fig.). Taken together, these results reinforce our confidence
301 in the proposed structural model and show that the HP1421 interaction with ComB4 is
302 essential for the functionality of the ComB system.
303 All the results presented so far indicate that HP1421 is indeed the VirB11 homologue
304 linked to the ComB T4SS. We therefore propose herein naming it ComB11.
305
306 **The association of ComB11 with the membrane is not dependent on ComB4.** The polar
307 localization of DotB E191K was dependent on DotO, the VirB4 orthologue[35]. In view of the
308 above results revealing the interaction between ComB11 and ComB4, we asked whether the
309 enrichment of ComB11 E176K at the membranes was affected by the absence of ComB4.
310 Western blots of the membrane and soluble fractions obtained from a *ΔcomB4* strain
311 expressing the mutant ComB11 showed the same distribution of the ATPase than in a ComB4
312 proficient strain (Fig. 6D) indicating that the interaction between the two ComB components
313 does not drive the association, possibly transient, of ComB11 with the inner membrane.
314
315 ***comB11* is a core gene in *H. pylori* whose Com system is recent.** To analyse the distribution
316 of the ComB system and how it relates to ComB11, we analysed the 364 completely

317 assembled genomes of *Helicobacteraceae* from RefSeq[42]. To be noted, 326 of these
318 genomes are from *H. pylori*. We first tested that the protein ComB11 in the focal strain
319 (26695) is sufficiently similar to the VirB11 protein profile of the T4SS model of TXSScan[43]
320 to be regarded as a *bona fide* homolog. This is indeed the case, since it was significantly
321 matched by the Virb11 protein profile of TXSScan (i-value=$8x10^{-39}$). We then took every
322 protein of the ComB system and searched for homologs in all the genomes of
323 *Helicobacteraceae* by sequence similarity using diamond blastp[44]. The results show that
324 most of the genes encoding ComB are very frequent in *H. pylori*. The least common genes
325 are the *comB7* homologs present in only 2/3rds of the genomes. It was previously observed
326 that *virB*7 genes are often missed in genome scans because the gene is small and evolves
327 fast[45]. The most common gene, and the only gene present in every single strain of *H.*
328 *pylori*, is *comB11* (Fig. 7B). We identified *bona fide* homologs of most of these genes in two
329 other *Helicobacteraceae*: *Helicobacter cetorum* and *Helicobacter acinonychis*, the two closest
330 species in the family for which we had complete genomes[46]. Systems associated with
331 natural transformation are known to be occasionally defective in strains of a species, *e.g.*
332 *comM* of *A. baumanni* was found to be defective or missing in more than 20% of the
333 strains[47]. Yet, when present, the components of orthologous systems are expected to have
334 similar genetic organisation. In the focal strain, the ComB system was split in three loci, one
335 locus with *comB2-B3-B4*, another locus ca. 20 genes apart with *comB6-B7-B8-B9-B10*, and
336 finally *comB11* which is distant from the others. We observed that the organization of each
337 locus is highly conserved. When genes were present, the two first loci were strictly
338 conserved in both *H. pylori* and the two close related species. Yet, relative distance between
339 the three loci is variable (Fig. 7C) and they are never contiguous (minimal distance between
340 the *comB4* and the *comB6* loci is 18 genes). The gene *comB11* was always distant from the
341 others, although in many genomes it is between 30 and 40 genes apart from the *comB6*
342 locus. Hence, the ComB system is present in most *H. pylori* strains and the two closest
343 species in a conserved genetic organization, suggesting that the acquisition of the system
344 predated the divergence of these three species.
345
346 **Figure 7**. **Frequency of the ComB system across *H. pylori*. A)** Typical organisation of the loci. **B)** frequency
347 of each gene in the strains of *H. pylori*. Only *comB11* is present in all the strains. **C)** Distances between key

genes of each of the tree loci (see A for reference). Distances are computed as the minimal circular distance between the genes, counting the number of intervening genes.

We have observed homologs of *comB* genes in species more distant from *H. pylori*. *Helicobacter heilmannii* (strain type) encodes homologs of *comB2-3-4-6-8-9-11* and *Helicobacter felis* ATCC 49179 has homologs of *comB2-3-4-6-9-9-10-11*. In both genomes the genes are scattered in different loci, albeit the loci are not similar to those of *H. pylori* (e.g. in *H. heilmannii* comB6 and comB8 are isolate and separated from the locus with *comB9-10*). These scattered loci are almost certainly not part of a conjugative system of an integrative conjugative element, where they are usually co-localised in one single locus[48]. Further work will be needed to test if they are driving natural transformation in these species. Yet, we have observed that all these genomes lack a homolog of the ComH protein with the N-terminal domain, which was shown to be absolutely required for transformation in *H. pylori*[49] and was only identified in this species, *Helicobacter cetorum* and *Helicobacter acinonychis*.

Discussion

During natural transformation, *H. pylori* can efficiently import double-stranded DNA from the milieu into the bacterial periplasm[12,25], where it is bound by the DNA receptor ComH[49]. While in other naturally transformable species characterised so far this process of capture and uptake of the tDNA is mediated by type IV pili or pilus-like structures[10], in *H. pylori* it relies on a T4SS, ComB[15,16,50]. This is a surprising finding since T4SSs are known as nanomachines that span a donor bacterium cell envelope to transfer macromolecules into target cells, whereas in the case of ComB it mediates the internalisation of the tDNA. Moreover, most T4SSs export proteins or DNA directly from the cytoplasm, while in *H. pylori* ComB delivers the incoming DNA into the periplasm, carrying out the first step of the two-step translocation mechanism mediating the passage of the DNA through the cell wall[25]. This process is completed by the transformation-specific ComH and ComEC proteins. ComH binds the DNA exiting ComB and delivers it to ComEC that, together with ComFC, allows the

380 passage of the DNA through the inner-membrane[46]. This unusual function, mediating the
381 uptake rather than the secretion of DNA, raises the question of how this particular T4SS
382 works. ComB components coded by the two *comB* operons previously described[15,16] point
383 to a minimised T4SS structure comparable to the canonical *A. tumefaciens* VirB system[51].
384 However, even for a minimized system, the lack of a VirB11 homologue in a Gram-negative
385 T4SS was puzzling[19]. The results presented above allowed the identification of this key
386 component of the ComB system required for the capture and uptake of DNA for natural
387 transformation of the *H. pylori*.
388 The work presented here indicates that from the structural and biochemical points of
389 view and the consequences of its inactivation, HP1421 is clearly a *bona fide* VirB11
390 homologue essential for the functioning of the T4SS ComB system. In accordance with the
391 proposal to unify the nomenclature of the conserved T4SS subunits[19] we propose to name
392 it ComB11.
393 In strain 26695 ComB11 is encoded by a gene distant from the two operons coding
394 for the rest of the ComB genes. Even if the distance to the other *comB* genes is variable, this
395 is true for all *H. pylori* strains for which assembled genomes are available. Since T4SSs are
396 usually encoded in a single locus, this suggests that after the system was acquired and co-
397 opted to participate in natural transformation, its encoding locus was split and relative
398 positions between the novel loci depend on the larger chromosomal rearrangements
399 frequently observed in the species[52]. Similar cases of secretion systems loci being split
400 have been identified before, but they are rare[53]. Amongst the *Helicobacteraceae* species
401 for which complete genomes are available, only two other, *Helicobacter cetorum* and
402 *Helicobacter acinonychis,* the closest to *H. pylori,* have a similar set of *comB* genes.
403 Interestingly, in those two strains, ComH, which is indispensable for *H. pylori* natural
404 transformation[49], displays the highest degree of homology with the *H. pylori* (74% and 58%
405 for *H. acinonychis* and *H. cetorum,* respectively) when compared to the other members of
406 the family. Moreover, for these two species closest to *H. pylori*, the alignment of the
407 homologs' sequences is along all the length of the protein while for the others it is limited to
408 the C-terminal region of ComH. Previous work showed that the N-terminal domain of ComH
409 is absolutely required for transformation[49]. Together these observations suggest that
410 *Helicobacteraceae* other than *H. pylori, H. acinonychis* and *H. cetorus* are either non-
411 transformable or use a system different than ComB/ComH.

412 Transcriptome analyses indicated that *hp1421* is downregulated in bacteria exposed
413 to low pH[54], similarly to what was observed for *comB8* and *comH*[55]. Interestingly,
414 development of competence requires an increase in pH of the culture[56,57]. The levels of
415 other ComB components were shown to be limiting for the transformation capacity of *H.*
416 *pylori*[58]. Our results thus suggest that the expression of ComB11 could impact *H. pylori*
417 transformation capacity by determining the availability of the tDNA uptake machinery.
418 Previous studies pointed to a potential association of HP1421 with *H. pylori* infection
419 capacity. Indeed, *hp1421* mutants were unable to colonise the stomach in a Mongolian gerbil
420 model[59]. Because *hp1421* is within a conserved operon harbouring genes involved in
421 flagellar synthesis and export, a defect in flagellum formation could explain the lack of
422 virulence provoked by the HP1421 absence. However, non-polar mutants of *hp1421*
423 displayed normal flagella and motility[60]. While a defect in natural transformation was
424 shown to affect *H. pylori* infection capacity in a mouse model[8], deletion of the *comB8-10*
425 operon did not impair gerbil colonisation[59]. These observations suggest that, besides its
426 essential role in natural transformation described in this work, HP1421 could have so far
427 undefined functions required for infection. Such a possibility is supported by our finding that
428 while *comB11* is a core gene present in all *H. pylori* strains, this is not the case for the other
429 *comB* genes.
430 What is ComB11 function within the ComB T4SS? It had been proposed that the
431 energy required for assembly and the retraction of a hypothetical pseudopilus capable of
432 binding DNA, and therefore deliver it into the periplasm, is provided solely by ComB4[19].
433 ComB11, through its enzymatic activity and its interaction with ComB4 would complete the
434 energy hub linked to the inner membrane complex. In other systems, the double-ring ATPase
435 complex (VirB4/11) generates the energy required for pilus biogenesis[61]. Consistently with
436 the lack of a VirB5 homologue which is required not only for adhesion of conjugative pili to
437 target cells, but also in the initiation of pilus extrusion from the cell[19,21], no pilus structure
438 associated with natural transformation has been described for *H. pylori.* However, the ComB
439 system does harbour a pilin homologue, ComB2. It is tempting to speculate that ComB4/11
440 provides the energy to extract ComB2 from the inner membrane to form a polymer capable
441 of reaching the surface of the cell where it could interact with a yet unidentified DNA-binding
442 protein (Fig. 8). In any case, energy is certainly required for the uptake of the transforming
443 DNA through the outer-membrane and into the periplasm. The ComB4/11 complex could

444 also provide such energy for the internalisation of the DNA through the retraction of a
445 pseudopilus structure formed by ComB2 (Fig. 8). T4SS pilus retraction has only been shown
446 for the system encoded by the F plasmid[62,63], but the mechanisms underlying this process
447 remain to be determined. A dual function implicating VirB11 as a switch between pilus
448 biogenesis and DNA transport has been proposed[64]. The finding of the VirB11 homologue
449 for the ComB T4SS provides a new model in which to analyse the role of these ATPases.
450
451 **Figure 8**. **Model for the ComB role during natural transformation.** See discussion section
452
453 **Materials and methods**
454 **Strains culture.** *Helicobacter pylori* 26695 strains listed on Supplementary Table 1 were
455 cultured on blood agar base (Millipore) or brucella broth base (Millipore) supplemented with
456 1,5% bacteriological agar (Sigma-Aldrich), both enriched with 10 % of horse defibrinated
457 blood (Thermo Scientific Oxoid). For liquid cultures, brain heart infusion (BHI) (Millipore)
458 media was supplemented with 10% heat-inactivated fetal calf serum (FCS) (Eurobio
459 scientific). All media were supplemented with an antimicrobial cocktail containing polymyxin
460 B (0.155 mg/ml), vancomycin (6.25 mg/ml), trimethoprim (3.125 mg/ml), and amphotericin
461 B (1.25 mg/ml) (all from Sigma/Sigma-Aldrich). Bacteria were grown at 37 °C under
462 microaerophilic conditions obtained with the Whitley Jar Gassing System (Don Whitley
463 scientific, United Kingdom) and a standardized gas mixture (3% O_2, 10% CO_2) (Air Products,
464 France) using agitation when required (150 rpm) (INFORS HT Ecotron-Switzerland). When
465 indicated, media were supplemented with kanamycin (20 µg/ml) (Sigma), apramycin
466 (12.5 µg/ml) (Sigma), chloramphenicol (8 µg/ml) (Fisher) and/or streptomycin (10 µg/ml)
467 (Sigma).
468 *Escherichia coli* strains used in this study are listed in Supplementary Table 2. Cultures used
469 were carried out in liquid or solid Lysogeny broth (LB-Sigma) supplemented with the
470 adequate antibiotic (ampicillin 100 µg/mL or kanamycin 50 µg/ml).
471 **Plasmid constructions.** Constructions for gene disruption or complementation in *H. pylori*
472 strains were carried out by using Sequence and Ligation Independent Cloning (SLIC)
473 reaction[65]. Simultaneous and independent PCR reactions were performed in order to
474 obtain an insert and a vector with overlapping sequences bigger than 18 bp. Briefly, 150 ng
475 of the purified vector were mixed with the insert following a 1:5 ratio, 2 µL of NEBuffer r2.1

476 (New England Biolabs), 0.25 µL of T4 DNA polymerase (New England Biolabs) and H_2O up to
477 a final volume of 20 µL. Sample was incubated at room temperature 6 min and reaction
478 stopped by using 2 µL of dCTP 10 mM, followed by a 15 min incubation at 37 °C. Right after 7
479 µL were used to transform 50 µL of chemo-competent DH5-α *E. coli* cells. Plasmids and
480 oligonucleotides used in this study are listed in supplementary Table 3 and 4 respectively.
481 ***H. pylori* gene inactivation.** Genomic sequences including 200 bp upstream and downstream
482 of the gene of interest (chr: 1490990 bp to 1491904 bp for *hp1421;* chr: 14248 bp to 16611
483 bp for *comB4*) were amplified by PCR and cloned in pJET 1.2 backbone using SLIC reaction. A
484 kanamycin non-polar cassette was used to replace the open reading frame for hp1421 gene
485 and apramycin for *comB4*. Reference sequences were obtained from
486 https://mage.genoscope.cns.fr/ *Helicobacter pylori* 26695 - chromosome NC_000915.1[66].
487 **Complementation.** pJET 1.2 plasmids containing loci *ureA* (Chr: 77653 bp to 78221 bp) or *rdx*
488 (Chr: 1013570 bp to 1014169) fused to the *comH* promoter (Chr: 1607419 bp to 1607618 bp)
489 in position 1013912 bp were used for *hp1421* ectopic complementation. For *ureA* locus, the
490 gene of interest was inserted on position 77956 bp. Alternatively, *hp1421* ORF was inserted
491 downstream of the *comH* promoter. For both constructs a chloramphenicol non-polar
492 cassette was inserted right after the gene. A FLAG tag was added at N-terminal side to follow
493 up expression. Regarding constructs to test interacting comB4 and hp1421 mutants, *comB4*
494 gene (Chr: 14248 bp to 16611 bp) was inserted on a pJET 1.2 plasmid containing loci *ureA*
495 (Chr: 77653 bp to 78221 bp) at position 77956 bp. Adjacent to the gene, the previous
496 described construct "*rdx*-p*comH* promoter-FLAG-*hp1421*-chloramphenicol cassette" was
497 fused. An Alfa-tag was added at C-terminal side of *comB4* to follow up expression. Different
498 *hp1421* and *comB4* gene variants were obtained by site directed mutagenesis[67] of these
499 plasmids. Introduction of the various constructs in *H. pylori* was carried out by natural
500 transformation or electroporation.
501 For natural transformation, plate-cultured *H. pylori* cells were taken to 4 OD_{600} in 40
502 µL of peptone water, containing 600 ng of plasmidic or genomic DNA harboring the construct
503 of interest. The mixture was spotted in two 20 µL aliquots on blood agar brucella and
504 incubated at 37 °C overnight in microaerophilic conditions. In some cases, complementation
505 of KO strains deficient for the first steps of transformation was performed by electroporation
506 (detailed in "*Helicobacter pylori* electroporation"). Grown spots were spread separately on
507 blood agar brucella plates supplemented with the corresponding antibiotic and incubated

508 until colonies were observed (4 to 6 days). Isolated colonies were transferred to new plates
509 as patches keeping always the selection to escalate the inoculum to finally spread over half
510 plate. Finally, a small fraction of cells was collected to extract gDNA by resuspension with 100
511 µL 50 mM NaOH followed by 20 minutes heating at 95 °C and a 5 minutes cooling with the
512 addition of 20 µL 1 M Tris-HCl pH 7. PCR verifications were performed by using Kit Taq'Ozyme
513 OneMix (Ozyme). For the complementing constructs, the genes were amplified using Q5
514 DNA high fidelity polymerase (New England Biolabs) and sequenced (Eurofins Genomics,
515 Cologne, Germany).
516 **Transformation efficiency tests.** Plate-cultured *H. pylori* strains were taken to OD_{600} = 4 in 45
517 µL final volume of peptone water, containing 600 ng of genomic DNA from a streptomycin
518 resistant 26695 strain. 15 µL aliquots were spotted by triplicate over blood agar brucella and
519 incubated overnight in microaerophilic conditions at 37 °C. Each spot was collected in 500 µl
520 of peptone water and decimal dilutions were performed (up to 10^{-6}). 10 µL aliquots were
521 spotted by triplicate on blood agar brucella plates in absence (dilutions 10^{-5} and 10^{-6}) or
522 presence of streptomycin (non-diluted to 10^{-3}). Plates were incubated until colonies
523 appeared and CFU/mL were calculated (n° of colonies * dilution factor * aliquot factor).
524 Transformation efficiency values were finally calculated by dividing the transformant CFU/mL
525 over the total number of bacteria.
526 ***H. pylori* electroporation.** Plate-cultured *H. pylori* cells were taken to OD_{600} = 10 in 1 mL final
527 volume of peptone water, pelleted and resuspended in 1 mL of sterile ice-cold
528 electrocompetent solution (9% sucrose - 15% glycerol). After centrifugation pellets were
529 resuspended in 250 µL electrocompetent solutionr and 1/5 of the reaction was transferred to
530 an electroporation cuvette and mixed with 600-1000 ng plasmidic or genomic DNA.
531 Electroporation was performed on ice, at 2.5 kV cm−1; 25 µF; 200 Ω (Gene Pulser II, Bio-Rad),
532 right after 100 µL of BHI were added and 50 µL spotted onto brucella blood agar plates.
533 **Subcellular fractionation.** Plate-cultured *H. pylori* cells were resuspended in peptone water.
534 Cells were washed once with sterile PBS (Gibco) 1X and normalized to OD_{600}= 10 in 1mL of
535 buffer A (Tris-HCl 10 mM pH 7.5 (Sigma); 1X protease inhibitor cocktail (cOmplete, Mini,
536 EDTA-free, Roche). Samples were sonicated on ice (amplitude 20%, 30s, 2s pulses, 2s
537 intervals) using a 3 mm microtip (Branson Digital Sonifier 450) and centrifuged 14000 g 15
538 min at 4°C (Eppendorf 5417R). The supernatant was collected and 100 µL were stored as
539 total extract. The remaining volume was ultra-centrifuged 119000 g 45min at 4°C (Beckman

540 Coulter Optima XPN-100), and supernatant was stored as soluble extract. The pellet
541 containing total membranes was washed using in 1 mL buffer A and centrifuged using the
542 same conditions as before. The pellet was resuspended in Buffer C (Tris-HCl 10 mM pH 7.5;
543 1X protease inhibitor cocktail; 1 % N-Lauroylsarcosine) to constitute the membrane fraction.
544 Protein identification in different bacterial compartments was done by western blot.
545 Additionally, as control of the experiment MotB (membrane marker) and NikR (cytoplasmic
546 marker) localization, was followed by using primary antibodies designed in rabbit and
547 secondary Goat-anti-rabbit IgG IR700 (Advansta).
548 **Western blots.** To verify protein expression in complemented strains, exponential phase
549 liquid cultures (18-24 h) were normalized at OD_{600} = 10 in 1 mL of 20 mM Tris-HCl pH 7.5 at
550 4°C (Sigma), 1X protease inhibitor (cOmplete, Mini, EDTA-free, Roche), right after samples
551 were sonicated on ice (amplitude 20%, 30s, 2s pulses, 2s intervals) using a 3 mm microtip
552 (Branson Digital Sonifier 450) and centrifuged 14000 g 10 min at 4°C (Eppendorf 5417R). 15
553 µL of extract were mixed with 5 µL of fresh Laemmli 4X, and heated 5 min at 95 °C for
554 HP1421 constructs and 50 °C 15 min for ComB4 ones. Total volume was loaded into 10-12%
555 hand-casted acrylamide gels (Mini-PROTEAN® Tetra 2-Gel, BioRad) and run using Mini-
556 PROTEAN Tetra Vertical Electrophoresis Cell at 0.75 A-150V-30W (PowerPac™ HC High-
557 Current Power Supply, BioRad) until running front was out. Resolved gels were transferred to
558 0.2µM nitrocellulose membranes (Trans-Blot Turbo Mini 0.2 µm Nitrocellulose Transfer
559 Packs, BioRad) using Mixed MW program on a Trans-Blot Turbo Transfer System (BioRad).
560 Membranes were blocked using 1X PBS, 0.3% Tween 20 (Sigma), 1% BSA (Sigma-Aldrich). For
561 FLAG-tagged proteins, a 1/5000 dilution of ANTI-FLAG M2 primary antibody produced in
562 mouse were used (Merck), and a 1/10000 dilution of secondary Goat-anti-mouse IgG IR800
563 (Advansta). Regarding ALFA-tag tagged proteins, a 1/1000 dilution of FluoTag®-X2 anti-ALFA
564 ATTO 488 antibodies designed in alpaca (NanoTag Biotechnologies) were used. Membranes
565 were washed with 1X PBS, 0.3% Tween 20 and revealed with iBright FL1500 (Thermo Fisher
566 Scientific).
567 **DNA Uptake.** Exponential phase liquid cultures (18-24 h) were normalized at OD_{600} = 1 in 1
568 mL of BHI-FCS. After a washing step using BHI sterile media, 250 ng of heterologous DNA
569 linear plasmid were added as donor to the standardized suspension in prewarmed BHI-FCS.
570 Samples were incubated 15 min at 37 °C in agitation (180 rpm) under microaerophilic
571 atmosphere. After incubation, suspensions were vortexed twice (2500 rpm/min) during 15 s

572 and centrifuged (8000 rpm- 3 min). Two washing cycles were performed using sterile PBS 1X
573 (Gibco), vortexing at high speed between each step. In order to eliminate free DNA, a
574 nuclease treatment was performed at 37 °C during 20 min by pellet resuspension in 500 µL
575 of a mixture containing 10 mM $MgCl_2$ (Merck), 50 UI/mL DNase I (Sigma) and 62.5 UI/mL
576 Benzonase (Millipore) in 1X PBS. This step was followed by high speed vortexing, pelleting
577 and 2 washing cycles as detailed before. Cells were resuspended in 200 µL of PBS 1X and 200
578 µL of phenol:chloroform:isoamyl alcohol (25:24:1) (Sigma) and vortexed 30 s at high speed.
579 Samples were centrifuged 12000 rpm for 1min and 100 µL of the upper phase were collected
580 in a new tube, after an equal volume of chloroform was added and DNA was extracted by
581 vortexing-centrifugation. Two simultaneous PCR reactions using Kit Taq'Ozyme OneMix
582 (Ozyme) were performed using oligos op284 and op285 to detect donor DNA (plasmid) and
583 Op31 and Op32 (Table XXXX) for recipient DNA (gDNA). Amplified fragments were resolved in
584 a 1% agarose gel stained with SYBR™ Safe (Invitrogen), and revealed with transillumination
585 (EBOX VX5/20M, Vilber Lourmat). After image acquisition, by using Fiji software band
586 intensity of each reaction was measured and background subtracted to obtain an absolute
587 valor, with those values a ratio recipient/donor was performed and internalization
588 percentages were calculated taking the wild-type strain as 100%.
589 **DNA foci detection.** *H. pylori* cells collected from blood agar plates were used to inoculate
590 BHI broth at OD_{600}= 0.05-0.1. When cultures reached exponential phase (18-24h), OD was
591 normalized to 4 in 20 µL and 200 ng of λ-DNA (New England Biolabs), labelled with Cy3 using
592 Label IT Nucleic Acid Labeling Kit (Mirus Bio) according to manufacturer instructions, were
593 added to the reaction. After 7 min at 37°C in agitation (150 rpm) and microaerophilic
594 conditions, cells were pelleted and washed with 100 µL of BHI media. In order to remove
595 free DNA, cell suspensions (50µL) were treated with 10 U DNase I (Sigma) 5 minutes at 37°C
596 followed by high speed vortexing. Bacteria were washed once more and resuspended in
597 20µL BHI, 3.5 µL of this suspension were spread on µ-Slide 8 Well (Ibidi) and 400 µL of soft
598 agar (BHI-FCS 1% agarose) was added to immobilize cells. 2D imaging was performed using
599 an inverted-confocal Nikon A1 microscope at 37°C (The Cube 2, Life Imaging Services), 10%
600 CO_2, 3% O_2 and 85% humidity (The Brick, Life Imaging Services); 100-x oil objective was used
601 and z-stack 0.125 µm acquisition 1248×1248-pixel resolution was carried out. Image
602 processing was done using ImageJ software. The used criteria included the manual counting
603 of entire rod shape cells and red foci over the cells in the composite image of bright field and

604 red channel (594 nm). After foci percentage were calculated (total n° of cells /n° of cells with
605 DNA foci).
606 **Protein purification.** *E. coli* BL21 (DE3) strains, transformed with pRSF duet containing N-
607 terminal 6His-MBP tags fused to hp1421 gene in wild type, E176A, E176K and R8D-R60E
608 versions, were cultured in 500 mL LB at an initial OD_{600} of 0.1 at 37°C in agitation (180 rpm).
609 At OD_{600}= 0.6-0.7, IPTG (Thermo Scientific) was added to 1 mM and cultures were incubated
610 overnight at 18°C in agitation. Cultures were centrifuged and pellets resuspended in buffer
611 500 mM NaCl (Sigma), 50 mM Tris-HCl (pH 8) (Sigma), 10% glycerol (Sigma-Aldrich), 1 mM
612 DTT (Sigma), 1 mg/mL lysozyme (Sigma), 1x cOmplete EDTA-free protease inhibitor (Roche).
613 The amount of buffer was calculated using the following formula: [(DO_{600} in 1 ml* total
614 volume of culture)/40]. After samples were sonicated on ice (amplitude 20%, 3min, 7s
615 pulses, 7s intervals) using a 13 mm tip probe (Branson Digital Sonifier 450). The protein of
616 interest was then purified from the soluble fraction, obtained by centrifugation at 20000 rpm
617 60 min at 4°C. 3 mL of equilibrated Ni-NTA Superflow resin (Qiagen) were incubated 3h at
618 4°C in agitation with the soluble fraction, right after the whole suspension was transferred to
619 a 2.5 × 10 cm Econo-Column (Bio-Rad), and flowthrough was obtained through pumping at
620 25 rpm (Mini peristaltic pump, Gilson). After, washing steps with 1.5 column volumes was
621 performed with buffer A (20 mM Tris pH8; 500 mM NaCl; 1 mM DTT; 10% glycerol; 20 mM
622 Imidazole), followed by 1.5 column volumes of buffer B (20 mM Tris pH8; 100 mM NaCl; 1
623 mM DTT; 10% glycerol; 20 mM Imidazole). Proteins were eluted in steps in 2 mL fractions
624 with: 20 mM Tris pH8; 100 mM NaCl; 1 mM DTT; 10% glycerol; 500 mM Imidazole. Purified
625 fractions were aliquoted, and stored at −80 °C.
626 **ATPase activity.** All tests were performed using the EnzChek® Phosphate Assay Kit (Molecular
627 probes, Invitrogen), following the protocol provided by the company. To determine HP1421
628 Michaelis constant (Km), a concentration rank of 0-4 mM ATP was used with a fixed amount
629 of protein. Briefly the reaction was incubated 30 min at 22 °C, and absorbance was read at
630 360 nm on a microplate reader (CLARIOstar – BGM Biotech). Released phosphate was
631 calculated by interpolation and corrected by subtraction of ATPase contamination
632 measurement in absence of ATP. Km values were calculated using nonlinear least squares
633 regression (GraphPad Prism 10.0.1). Regarding specific activity determinations on HP1421
634 R8DR60E mutants, phosphate release was followed on 5 minutes intervals during 45 min at
635 37 °C in a rank of 1-10 µM of protein at a fixed 4 mM concentration of ATP. Obtained values

636 were corrected as indicated before, and plotted in function of time, common linear intervals
637 were selected and slopes calculated. Finally, the slope of slope versus protein concentration
638 graph was calculated for each determined genotype.
639 **Bacterial two hybrid assay.** T25-*hp1421* and T18-*hp1421* constructs designed in plasmids
640 pKT25 and pUT18C (Euromedex) variants were co-transformed *E. coli* BTH101
641 chemocompetent cells. Two to three transformant colonies were resuspended in 100 µl of
642 LB, and 10 µL were spotted on solid LB supplemented with 100 µg/mL Ampicillin, 50 µg/mL
643 Kanamycin, 0.5 mM IPTG (Sigma) and 40 µg/mL X-gal (Roche). Plates were incubated at 30 °C
644 24h and images registered.
645 **Split luciferase constructs and tests.** *comB4* gene (Chr: 14248 bp to 16611 bp) was inserted
646 on a pJET 1.2 plasmid containing loci *ureA* (Chr: 77653 bp to 78221 bp) at position 77956 bp.
647 Adjacent to this gene the construct "*comH* promoter (Chr: 1607419 bp to 1607618 bp),
648 *hp1421* gene (chr: 1490990 bp to 1491904), chloramphenicol cassette" was added. Nano-
649 luciferase optimized fragment sequences for *H. pylori* expression Sm-Bit and Lg-Bit[68] were
650 fused to N-terminal hp1421 and C-terminal ComB4 respectively. Random 15 bp linkers were
651 added between the segments and gene sequences to allow flexibility. Different *hp1421* and
652 *comB4* gene variants were obtained by site directed mutagenesis of these plasmids. All
653 luciferase tests were performed using the Nano-Glo® Luciferase Assay System (Promega).
654 Briefly, plate-cultured *H. pylori* cells were taken to OD_{600} = 0.1 in BHI. 50 µL of each
655 suspension were mixed with 50 µL of reconstituted reaction buffer, by duplicate in Nunc F96
656 MicroWell White Polystyrene Plates (Thermo Scientific). Plate was gently mixed by tapping
657 and 3 minutes after, readings were performed each 30s up to 5 minutes final using a
658 microplate reader (CLARIOstar – BGM Biotech). Averaged blank corrected values were
659 summed and corrected by OD to normalize. To each replicate, wild type non-specific activity
660 was subtracted to each condition.
661 **AlphaFold modelling.** Most structural models were obtained using the AlphaFold3 web
662 server[30]. HP1421 hexamer with ATP, HP1421-ComB4, ComB4 hexamer were modeled with
663 full-length proteins. The HP1421/ComB4 double hexamer was modeled with shorter
664 delimitations due to AlphaFold3 size limit: only the C-terminal domain of ComB4 was used
665 (from the UniProt sequence reference O24862, residues 399-787 (end)). The HP1421-ComB4
666 interface was also modeled with AlphaFold2[39] using the ColabFold[40]implementation.

667 **Structural data visualization.** Molecular graphics and analyses performed with the UCSF
668 ChimeraX software[69], developed by the Resource for Biocomputing, Visualization, and
669 Informatics at the University of California, San Francisco, with support from National
670 Institutes of Health R01-GM129325 and the Office of Cyber Infrastructure and
671 Computational Biology, National Institute of Allergy and Infectious Diseases. The command
672 line version of matchmaker module was used to align protein chains and obtain RMSD values
673 with 5.0 Å pruning iteration cut-off distance (to exclude outlier atoms). The "pair ss"
674 parameter were applied when aligning complexes (hexamers) to ensure a global alignment
675 instead of a single pair based one. The electrostatic potential at HP1421-ComB4 interface
676 was estimated using ChimeraX "electrostatic" (coulombic) module. The plDDT colouring was
677 obtained directly from AlphaFold plDDT values in the json output file.
678 **Size exclusion chromatography.** The oligomerization state of the protein is determined by
679 passage through a Superdex 200 column. Calibration of the gel filtration column is performed
680 using a cocktail of eight proteins: aprotinin (6.5 kDa), ribonuclease A (13.7 kDa), carbonic
681 anhydrase (29 kDa), ovalbumin (44 kDa), conalbumin (75 kDa), aldolase (158 kDa), ferritin
682 (440 kDa), and thyroglobulin (669 kDa). The column is equilibrated with 20 mM Tris-HCl, pH
683 8.0, 100 mM NaCl, 1 mM DTT, and 10% glycerol. The purified protein (100 µg) is loaded onto
684 the column, and the elution volume of the protein is determined. By plotting this value on
685 the column calibration curve, the apparent molecular weight of the protein is calculated.
686 **Phylogenetic analyses.** We extracted from RefSeq complete genomes[42] (S5 file) all the 364
687 genomes of *Helicobacteraceae* (last accessed in May 2023). We used the annotations of the
688 genomes regarding the position of every protein coding gene and their functional
689 annotation. We used the proteins of the focal strain (26695) to identify homologs in the
690 other genomes using diamond blastp v2.0.4.142[44] with the *ultra-sensitive* option. Within
691 the closely related species of *H. pylori, Helicobacter cetorum* and *Helicobacter acinonychis*
692 we regarded proteins as orthologous if they were more than 80% identical. This threshold
693 was verified upon the analysis of the loci loci, by comparing the hits with this threshold with
694 those using a much lower threshold (e-value <0.001, down to less than 30% identity). This
695 confirmed that only homologs at more than 80% identity are found in the loci. Once the list
696 of orthologs was available we computed the minimal distance of each pair in the genome as
697 the number of genes that were identified between them (accounting for the circularity of the
698 genomes).

The test that comB11 is a *bona fide* virB11 homolog was done by checking that it can be identified by the virB11 HMM protein profile from TXSScan[43], using hmmsearch 3.1b2 with default options[70]. The protein profile is given in S6 File.

Statistical analysis. Independent experiments were performed using a completely randomized design with at least three biological replicates. RStudio software and Graphad Prism 10 were used to perform statistical analysis. Each dataset was analyzed using one way ANOVA and Tukey's test at $P < 0.05$. Model assumptions were verified using Shapiro–Wilk and Levene's tests, including Normal Q-Q- plot and residuals versus fits plot analysis. When residuals normality and homoscedasticity was not proven, boxcox function was used to choose the best data transformation. If assumptions weren't still verified, non-parametrical Kruskal and Wallis test followed by post-hoc SNK test at $P<0.05$ (global P value adjusted to the number of comparisons) was performed.

Data availability

All relevant data are available within the main text, the supporting information files and on Zenodo (https://doi.org/10.5281/zenodo.19238504). Data used for graphs and tables are available as a Data Source file. All other data can be requested to the authors.

References

1. Good BH, Zuckerberg Biohub-San C, Mcdonald MJ, Ami), Bhatt S, Mcdonald MJ. Unraveling the tempo and mode of horizontal gene transfer in bacteria. Trends Microbiol. 2025;33: 853–865. doi:10.1016/J.TIM.2025.03.009
2. Arnold BJ, Huang IT, Hanage WP. Horizontal gene transfer and adaptive evolution in bacteria. Nature Reviews Microbiology 2021 20:4. 2021;20: 206–218. doi:10.1038/S41579-021-00650-4
3. Soucy SM, Huang J, Gogarten JP. Horizontal gene transfer: building the web of life. Nat Rev Genet. 2015;16: 472–482. doi:10.1038/nrg3962
4. Woods LC, Gorrell RJ, Taylor F, Connallon T, Kwok T, McDonald MJ. Horizontal gene transfer potentiates adaptation by reducing selective constraints on the spread of genetic variation. Proc Natl Acad Sci U S A. 2020;117: 26868–26875. doi:10.1073/pnas.2005331117
5. Suerbaum S, Achtman M. Evolution of Helicobacter pylori: the role of recombination. Trends Microbiol. 1999;7: 182–184. Available: http://www.ncbi.nlm.nih.gov/entrez/query.fcgi?cmd=Retrieve&db=PubMed&dopt=Citation&list_uids=10383222
6. Suerbaum S, Smith JM, Bapumia K, Morelli G, Smith NH, Kunstmann E, et al. Free recombination within Helicobacter pylori. Proc Natl Acad Sci U S A. 1998;95: 12619–12624. Available: http://www.ncbi.nlm.nih.gov/entrez/query.fcgi?cmd=Retrieve&db=PubMed&dopt=Citation&list_uids=9770535

7. Fischer W, Windhager L, Rohrer S, Zeiller M, Karnholz A, Hoffmann R, et al. Strain-specific genes of Helicobacter pylori: genome evolution driven by a novel type IV secretion system and genomic island transfer. Nucleic Acids Res. 2010;38: 6089–6101. doi:10.1093/nar/gkq378
8. Dorer MS, Cohen IE, Sessler TH, Fero J, Salama NR. Natural Competence Promotes Helicobacter pylori Chronic Infection. Blanke SR, editor. Infect Immun. 2013;81: 209–215. doi:10.1128/IAI.01042-12
9. Suerbaum S, Ailloud F. Genome and population dynamics during chronic infection with Helicobacter pylori. Current Opinion in Immunology. 2023. doi:10.1016/j.coi.2023.102304
10. Dubnau D, Blokesch M. Mechanisms of DNA Uptake by Naturally Competent Bacteria. Annual Review of Genetics. 2019. pp. 217–237. doi:10.1146/annurev-genet-112618-043641
11. Johnston C, Martin B, Fichant G, Polard P, Claverys JP. Bacterial transformation: distribution, shared mechanisms and divergent control. Nat Rev Microbiol. 2014;12: 181–196. doi:10.1038/nrmicro3199
12. Kruger NJ, Stingl K. Two steps away from novelty--principles of bacterial DNA uptake. Mol Microbiol. 2011;80: 860–867. doi:10.1111/j.1365-2958.2011.07647.x
13. Seitz P, Blokesch M. DNA transport across the outer and inner membranes of naturally transformable Vibrio cholerae is spatially but not temporally coupled. mBio. 2014;5. doi:10.1128/mBio.01409-14
14. Damke PP, Celma L, Kondekar SM, Di Guilmi AM, Marsin S, Dépagne J, et al. ComFC mediates transport and handling of single-stranded DNA during natural transformation. Nat Commun. 2022;13. doi:10.1038/S41467-022-29494-Z
15. Hofreuter D, Odenbreit S, Haas R. Natural transformation competence in Helicobacter pylori is mediated by the basic components of a type IV secretion system. Mol Microbiol. 2001;41: 379–391. Available: http://www.ncbi.nlm.nih.gov/entrez/query.fcgi?cmd=Retrieve&db=PubMed&dopt=Citation&list_uids=11489125
16. Karnholz A, Hoefler C, Odenbreit S, Fischer W, Hofreuter D, Haas R. Functional and topological characterization of novel components of the comB DNA transformation competence system in Helicobacter pylori. J Bacteriol. 2006;188: 882–893. doi:10.1128/JB.188.3.882-893.2006/ASSET/8DA3B1D6-B276-45C2-9752-C4AD8583D250/ASSETS/GRAPHIC/ZJB0030654120006.JPEG
17. Denise R, Abby SS, Rocha EPC. The Evolution of Protein Secretion Systems by Co-option and Tinkering of Cellular Machineries. Trends Microbiol. 2020;28: 372–386. doi:10.1016/J.TIM.2020.01.005
18. Guglielmini J, De La Cruz F, Rocha EPC. Evolution of Conjugation and Type IV Secretion Systems. Mol Biol Evol. 2013;30: 315–331. doi:10.1093/MOLBEV/MSS221
19. Christie PJ, Waksman G, Berntsson RP-A, Soler N, Leblond-Bourget N, Douzi B. Type IV secretion systems: reconciling diversity through a unified nomenclature. FEMS Microbiol Rev. 2026;50. doi:10.1093/femsre/fuaf069
20. Smeets LC, Kusters JG. Natural transformation in Helicobacter pylori: DNA transport in an unexpected way. Trends Microbiol. 2002;10: 159–62; discussion 162. Available: http://www.ncbi.nlm.nih.gov/entrez/query.fcgi?cmd=Retrieve&db=PubMed&dopt=Citation&list_uids=11912014
21. Paillard P, Rouger Q, Thomet M, Macé K. Type IV secretion systems: from structures to mechanisms. The EMBO Journal 2025 44:22. 2025;44: 6304–6319. doi:10.1038/S44318-025-00584-0
22. Karnholz A, Hoefler C, Odenbreit S, Fischer W, Hofreuter D, Haas R. Functional and topological characterization of novel components of the comB DNA transformation competence system in Helicobacter pylori. J Bacteriol. 2006;188: 882–893. doi:10.1128/JB.188.3.882-893.2006
23. Suckow G, Seitz P, Blokesch M. Quorum sensing contributes to natural transformation of Vibrio cholerae in a species-specific manner. J Bacteriol. 2011;193: 4914–4924. doi:10.1128/JB.05396-11
24. Seitz P, Pezeshgi Modarres H, Borgeaud S, Bulushev RD, Steinbock LJ, Radenovic A, et al. ComEA Is Essential for the Transfer of External DNA into the Periplasm in Naturally Transformable Vibrio cholerae Cells. PLoS Genet. 2014;10: e1004066. doi:10.1371/journal.pgen.1004066

25. Stingl K, Müller S, Scheidgen-Kleyboldt G, Clausen M, Maier B. Composite system mediates two-step DNA uptake into Helicobacter pylori. Proc Natl Acad Sci U S A. 2010;107: 1184–1189. doi:10.1073/PNAS.0909955107
26. Corbinais C, Mathieu A, Kortulewski T, Radicella JP, Marsin S. Following transforming DNA in Helicobacter pylori from uptake to expression. Mol Microbiol. 2016;101: 1039–1053. doi:10.1111/mmi.13440
27. Stingl K, Müller S, Scheidgen-Kleyboldt G, Clausen M, Maier B. Composite system mediates two-step DNA uptake into Helicobacter pylori. Proc Natl Acad Sci U S A. 2010;107. doi:10.1073/pnas.0909955107
28. Arya T, Oudouhou F, Casu B, Bessette B, Sygusch J, Baron C. Fragment-based screening identifies inhibitors of ATPase activity and of hexamer formation of Cagα from the Helicobacter pylori type IV secretion system. Sci Rep. 2019;9. doi:10.1038/s41598-019-42876-6
29. Ripoll-Rozada J, García-Cazorla Y, Getino M, Machón C, Sanabria-Ríos D, de la Cruz F, et al. Type IV traffic ATPase TrwD as molecular target to inhibit bacterial conjugation. Mol Microbiol. 2016;100. doi:10.1111/mmi.13359
30. Abramson J, Adler J, Dunger J, Evans R, Green T, Pritzel A, et al. Accurate structure prediction of biomolecular interactions with AlphaFold 3. Nature. 2024;630: 493–500. doi:10.1038/S41586-024-07487-W,
31. Rashkova S, Spudich GM, Christie PJ. Characterization of membrane and protein interaction determinants of the Agrobacterium tumefaciens VirB11 ATPase. J Bacteriol. 1997;179: 583–591. doi:10.1128/JB.179.3.583-591.1997
32. Christie PJ, Ward JE, Gordon MP, Nester EW. A gene required for transfer of T-DNA to plants encodes an ATPase with autophosphorylating activity. Proc Natl Acad Sci U S A. 1989;86. doi:10.1073/pnas.86.24.9677
33. Kutter S, Buhrdorf R, Haas J, Schneider-Brachert W, Haas R, Fischer W. Protein subassemblies of the Helicobacter pylori cag type IV secretion system revealed by localization and interaction studies. J Bacteriol. 2008;190. doi:10.1128/JB.01341-07
34. Sexton AA, Yeo H-J, Vogel JP, Sexton JA, Yeo H-J, Vogel JP. Genetic analysis of the Legionella pneumophila DotB ATPase reveals a role in type IV secretion system protein export. Mol Microbiol. 2005;57: 70–84. doi:10.1111/J.1365-2958.2005.04667.X
35. Chetrit D, Hu B, Christie PJ, Roy CR, Liu J. A unique cytoplasmic ATPase complex defines the Legionella pneumophila type IV secretion channel. Nature Microbiology 2018 3:6. 2018;3: 678–686. doi:10.1038/S41564-018-0165-Z
36. Macé K, Vadakkepat AK, Redzej A, Lukoyanova N, Oomen C, Braun N, et al. Cryo-EM structure of a type IV secretion system. Nature 2022. 2022; 1–6. doi:10.1038/s41586-022-04859-y
37. Scheibner F. Functional characterization of VirB/VirD4 and Icm/Dot type IV secretion systems from the plant-pathogenic bacterium Xanthomonas euvesicatoria. Front Cell Infect Microbiol. 2023;13: 1203159. doi:10.3389/FCIMB.2023.1203159/BIBTEX
38. Hu B, Khara P, Song L, Lin AS, Frick-Cheng AE, Harvey ML, et al. In Situ Molecular Architecture of the Helicobacter pylori Cag Type IV Secretion System. mBio. 2019;10. doi:10.1128/MBIO.00849-19
39. Jumper J, Evans R, Pritzel A, Green T, Figurnov M, Ronneberger O, et al. Highly accurate protein structure prediction with AlphaFold. Nature 2021 596:7873. 2021;596: 583–589. doi:10.1038/s41586-021-03819-2
40. Mirdita M, Schütze K, Moriwaki Y, Heo L, Ovchinnikov S, Steinegger M. ColabFold: making protein folding accessible to all. Nat Methods. 2022;19: 679–682. doi:10.1038/s41592-022-01488-1
41. Savvides SN, Yeo HJ, Beck MR, Blaesing F, Lurz R, Lanka E, et al. VirB11 ATPases are dynamic hexameric assemblies: new insights into bacterial type IV secretion. EMBO J. 2003;22: 1969–1980. doi:10.1093/EMBOJ/CDG223
42. Haft DH, DiCuccio M, Badretdin A, Brover V, Chetvernin V, O'Neill K, et al. RefSeq: an update on prokaryotic genome annotation and curation. Nucleic Acids Res. 2018;46: D851–D860. doi:10.1093/nar/gkx1068
43. Abby SS, Cury J, Guglielmini J, Néron B, Touchon M, Rocha EPC. Identification of protein secretion systems in bacterial genomes. Sci Rep. 2016;6. doi:10.1038/srep23080

44. Buchfink B, Xie C, Huson DH. Fast and sensitive protein alignment using DIAMOND. Nat Methods. 2015;12: 59–60. doi:10.1038/nmeth.3176
45. Guglielmini J, De La Cruz F, Rocha EPC. Evolution of Conjugation and Type IV Secretion Systems. Mol Biol Evol. 2013;30: 315–331. doi:10.1093/MOLBEV/MSS221
46. Mitchell HM, Rocha GA, Kaakoush NO, O'Rourke JL, Queiroz DMM. The Family Helicobacteraceae. In: Rosenberg E, DeLong EF, Lory S, Stackebrandt E, Thompson F, editors. The Prokaryotes. Berlin, Heidelberg: Springer Berlin Heidelberg; 2014. pp. 337–392. doi:10.1007/978-3-642-39044-9_275
47. Mazzamurro FI, Baby Chirakadavil J, Durieux I, Poiré L, Plantade J, Ginevra C, et al. Intragenomic conflicts with plasmids and chromosomal mobile genetic elements drive the evolution of natural transformation within species. de Visser JAGM, editor. PLoS Biol. 2024;22: e3002814. doi:10.1371/JOURNAL.PBIO.3002814
48. Cury J, Touchon M, Rocha EPC. Integrative and conjugative elements and their hosts: composition, distribution and organization. Nucleic Acids Res. 2017;45: 8943–8956. doi:10.1093/nar/gkx607
49. Damke PP, Di Guilmi AM, Fernández Varela P, Velours C, Marsin S, Veaute X, et al. Identification of the periplasmic DNA receptor for natural transformation of Helicobacter pylori. Nat Commun. 2019;10: 1–11. doi:10.1038/s41467-019-13352-6
50. Hofreuter D, Odenbreit S, Henke G, Haas R. Natural competence for DNA transformation in Helicobacter pylori : identification and genetic characterization of the comB locus. Mol Microbiol. 1998;28: 1027–1038. doi:10.1046/J.1365-2958.1998.00879.X
51. Costa TRD, Patkowski JB, Macé K, Christie PJ, Waksman G. Structural and functional diversity of type IV secretion systems. Nature Reviews Microbiology 2023 22:3. 2023;22: 170–185. doi:10.1038/S41579-023-00974-3
52. Noureen M, Kawashima T, Arita M. Genetic Markers of Genome Rearrangements in Helicobacter pylori. Microorganisms. 2021;9: 621. doi:10.3390/microorganisms9030621
53. Denise R, Abby SS, Rocha EPC. Diversification of the type IV filament superfamily into machines for adhesion, protein secretion, DNA uptake, and motility. PLoS Biol. 2019;17: e3000390. doi:10.1371/JOURNAL.PBIO.3000390
54. Wen Y, Marcus EA, Matrubutham U, Gleeson MA, Scott DR, Sachs G. Acid-adaptive genes of Helicobacter pylori. Infect Immun. 2003;71: 5921–5939. doi:10.1128/IAI.71.10.5921-5939.2003;WGROUP:STRING:PUBLICATION
55. Bury-Moné S, Thiberge JM, Contreras M, Maitournam A, Labigne A, De Reuse H. Responsiveness to activity via metal ion regulators mediates virulense in the gastric pathogen Helicobacter pylori. Mol Microbiol. 2004;53: 623–638. doi:10.1111/J.1365-2958.2004.04137.X;WGROUP:STRING:PUBLICATION
56. Moore ME, Lam A, Bhatnagar S, Solnick J V. Environmental Determinants of Transformation Efficiency in Helicobacter pylori. J Bacteriol. 2014;196: 337–344. doi:10.1128/JB.00633-13
57. Krüger NJ, Knüver MT, Zawilak-Pawlik A, Appel B, Stingl K. Genetic Diversity as Consequence of a Microaerobic and Neutrophilic Lifestyle. PLoS Pathog. 2016;12: 1–24. doi:10.1371/journal.ppat.1005626
58. Corbinais C, Mathieu A, Damke PP, Kortulewski T, Busso D, Prado-Acosta M, et al. ComB proteins expression levels determine Helicobacter pylori competence capacity. 2017. doi:10.1038/srep41495
59. Kavermann H, Burns BP, Angermuller K, Odenbreit S, Fischer W, Melchers K, et al. Identification and characterization of Helicobacter pylori genes essential for gastric colonization. J Exp Med. 2003;197: 813–822. doi:10.1084/jem.20021531
60. Porwollik S, Noonan B, O'Toole PW. Molecular characterization of a flagellar export locus of Helicobacter pylori. Infect Immun. 1999;67: 2060–2070. doi:10.1128/IAI.67.5.2060-2070.1999;PAGE:STRING:ARTICLE/CHAPTER
61. Hospenthal MK, Costa TRD, Waksman G. A comprehensive guide to pilus biogenesis in Gram-negative bacteria. Nature Reviews Microbiology. 2017. doi:10.1038/nrmicro.2017.40
62. Goldlust K, Ducret A, Halte M, Dedieu-Berne A, Erhardt M, Lesterlin C. The F pilus serves as a conduit for the DNA during conjugation between physically distant bacteria. Proc Natl Acad Sci U S A. 2023;120. doi:10.1073/PNAS.2310842120/-/DCSUPPLEMENTAL

63. Clarke M, Maddera L, Harris RL, Silverman PM. F-pili dynamics by live-cell imaging. Proc Natl Acad Sci U S A. 2008;105. doi:10.1073/pnas.0806786105
64. Ripoll-Rozada J, Zunzunegui S, de la Cruz F, Arechaga I, Cabezón E. Functional Interactions of VirB11 Traffic ATPases with VirB4 and VirD4 Molecular Motors in Type IV Secretion Systems. J Bacteriol. 2013;195: 4195–4201. doi:10.1128/JB.00437-13/ASSET/C2933D45-2055-4F32-967C-D87FC83821B7/ASSETS/GRAPHIC/ZJB9990927860005.JPEG
65. Jeong JY, Yim HS, Ryu JY, Lee HS, Lee JH, Seen DS, et al. One-Step Sequence- and Ligation-Independent Cloning as a Rapid and Versatile Cloning Method for Functional Genomics Studies. Appl Environ Microbiol. 2012;78: 5440–5443. doi:10.1128/AEM.00844-12
66. Tomb JF, White O, Kerlavage AR, Clayton RA, Sutton GG, Fleischmann RD, et al. The complete genome sequence of the gastric pathogen Helicobacter pylori. Nature. 1997;388: 539–547. doi:10.1038/41483
67. Liu H, Naismith JH. An efficient one-step site-directed deletion, insertion, single and multiple-site plasmid mutagenesis protocol. BMC Biotechnology 2008 8:1. 2008;8: 91-. doi:10.1186/1472-6750-8-91
68. Grote A, Hiller K, Scheer M, Münch R, Nörtemann B, Hempel DC, et al. JCat: a novel tool to adapt codon usage of a target gene to its potential expression host. Nucleic Acids Res. 2005;33: W526–W531. doi:10.1093/nar/gki376
69. Meng EC, Goddard TD, Pettersen EF, Couch GS, Pearson ZJ, Morris JH, et al. UCSF ChimeraX: Tools for structure building and analysis. Protein Science. 2023;32: e4792. doi:10.1002/pro.4792
70. Eddy SR. Accelerated Profile HMM Searches. PLoS Comput Biol. 2011;7. doi:10.1371/journal.pcbi.1002195

Acknowledgements

We thank Anne Marie Di Guilmi for the initial construction of the plasmids used for the BACTH assays, Laurent Terradot (CNRS, Lyon) for sharing plasmids with us and Hilde De Reuse (Institut Pasteur, Paris) for antibodies against NikR and MotB. We thank the BIOI2 core facility for making the ColabFold pipeline easily accessible at the I2BC to run AlphaFold2.

Author contributions

Conceptualisation: JFV, JPR

Methodology: YF, RG, JA

Formal analysis: JFV, EPCR, YF, RG, JA

Investigation: JFV, SK, MM, CL, XV

Writing - Original Draft: JFV, JPR, EPCR, YF, JA

Writing – Review and Editing: JFV, SK, XV, EPCR, JPR, YF, RG, JA. All authors read and approved the manuscript.

Visualisation: JFV, JPR, YF

Supervision: JPR, JA

Project administration: JPR

Funding acquisition: JA, RG, JPR

Competing interests: The authors declare that they have no competing interests.

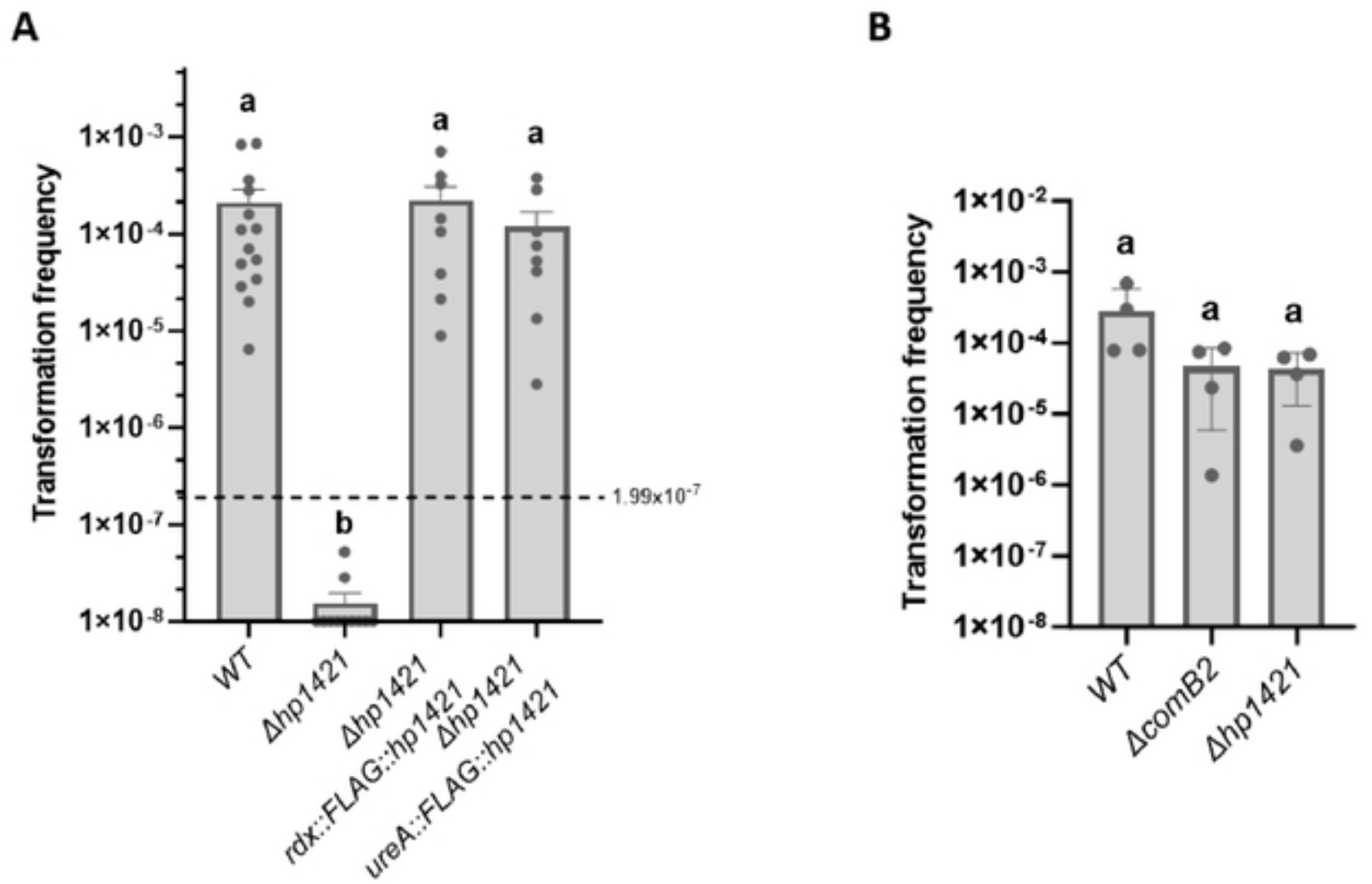
A
Transformation frequency
1×10-3
1×10-4
1×10-5
1×10-6
1×10-7
1×10-8
1.99×10-7
a
b
a
a
WT
Δhp1421
Δhp1421
rdx::FLAG::hp1421
Δhp1421
ureA::FLAG::hp1421
B
Transformation frequency
1×10-2
1×10-3
1×10-4
1×10-5
1×10-6
1×10-7
1×10-8
a
a
a
WT
ΔcomB2
Δhp1421

Figure 1.

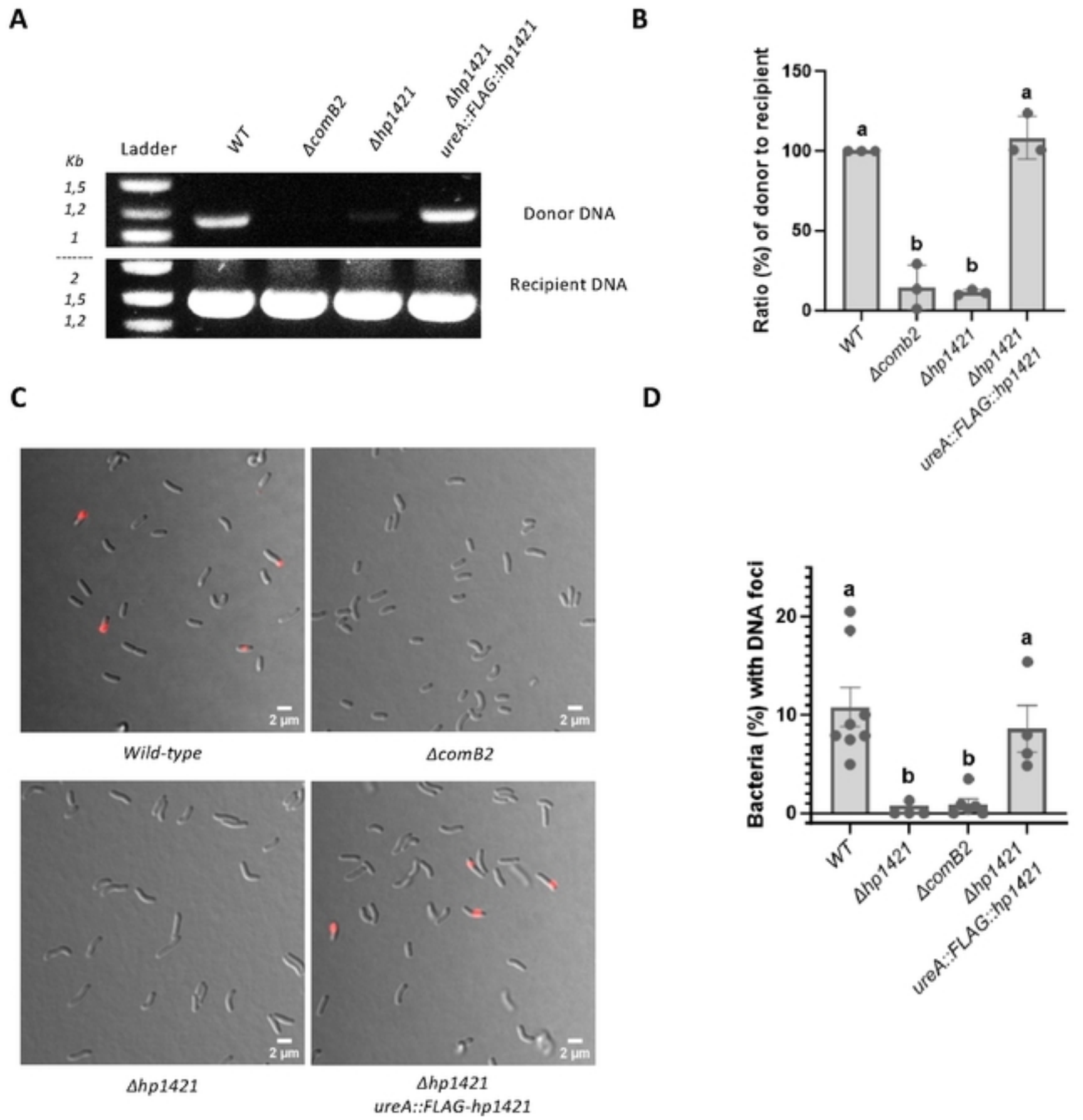
A
Ladder
WT
ΔcomB2
Δhp1421
Δhp1421 ureA::FLAG::hp1421
Kb
1,5
1,2
1
2
1,5
1,2
Donor DNA
Recipient DNA
B
Ratio (%) of donor to recipient
150
100
50
0
a
b
b
a
WT
Δcomb2
Δhp1421
Δhp1421 ureA::FLAG::hp1421
C
2 µm
Wild-type
ΔcomB2
Δhp1421
Δhp1421 ureA::FLAG-hp1421
D
Bacteria (%) with DNA foci
20
10
0
a
b
b
a
WT
Δhp1421
ΔcomB2
Δhp1421 ureA::FLAG::hp1421

Figure 2.

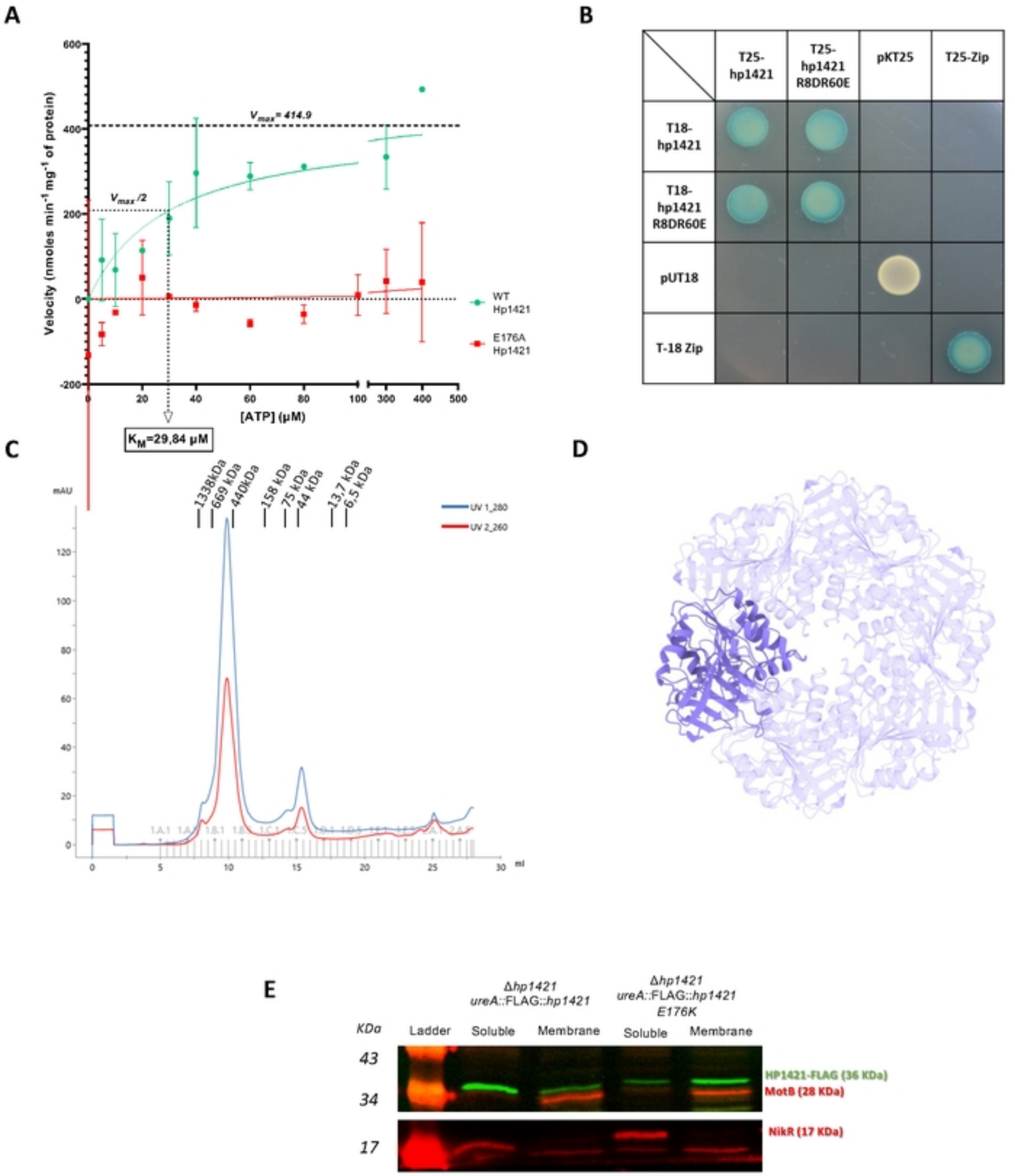
A
Velocity (nmoles min-1 mg-1 of protein)
Vmax = 414.9
Vmax /2
[ATP] (µM)
KM=29,84 µM
WT Hp1421
E176A Hp1421
B
T25-hp1421
T25-hp1421 R8DR60E
pKT25
T25-Zip
T18-hp1421
T18-hp1421 R8DR60E
pUT18
T-18 Zip
C
mAU
1338kDa
669 kDa
440kDa
158 kDa
75 kDa
44 kDa
13,7 kDa
6,5 kDa
UV 1_280
UV 2_260
ml
D
E
Δhp1421 ureA::FLAG::hp1421
Δhp1421 ureA::FLAG::hp1421 E176K
KDa
Ladder
Soluble
Membrane
Soluble
Membrane
43
34
17
HP1421-FLAG (36 KDa)
MotB (28 KDa)
NikR (17 KDa)

Figure 3.

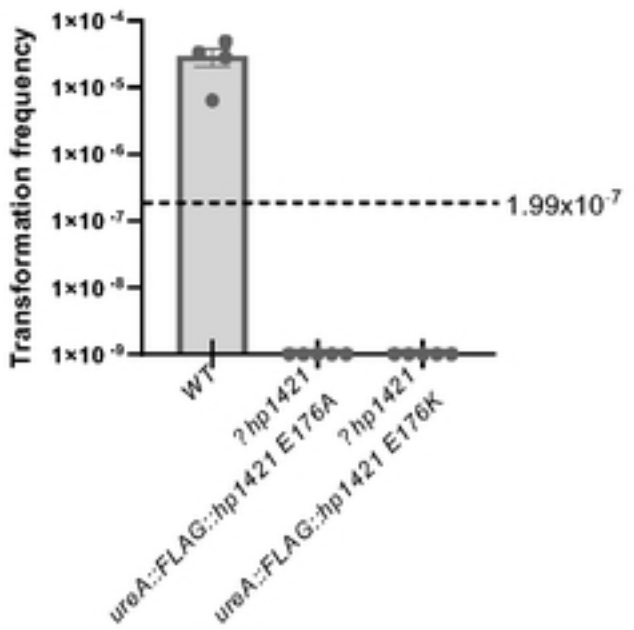
A
Transformation frequency
1×10⁻⁴
1×10⁻⁵
1×10⁻⁶
1×10⁻⁷
1×10⁻⁸
1×10⁻⁹
1.99x10⁻⁷
WT
?hp1421
ureA::FLAG::hp1421 E176A
?hp1421
ureA::FLAG::hp1421 E176K

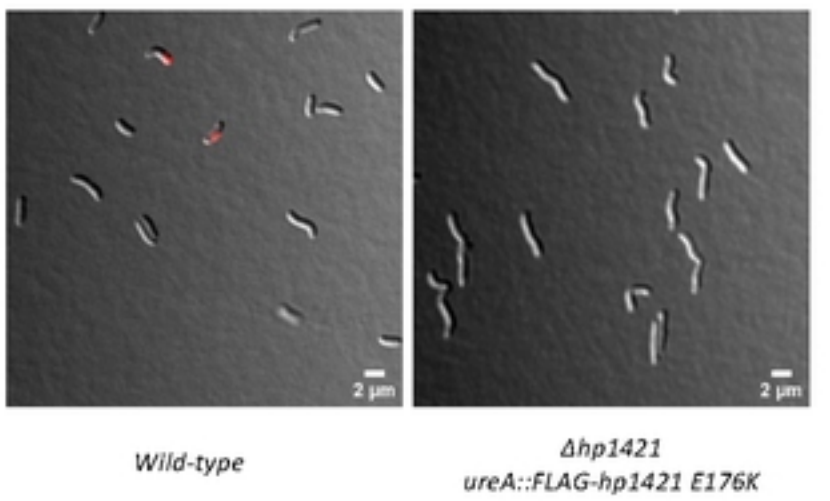
B
2 µm
2 µm
Wild-type
Δhp1421
ureA::FLAG-hp1421 E176K

Figure 4.

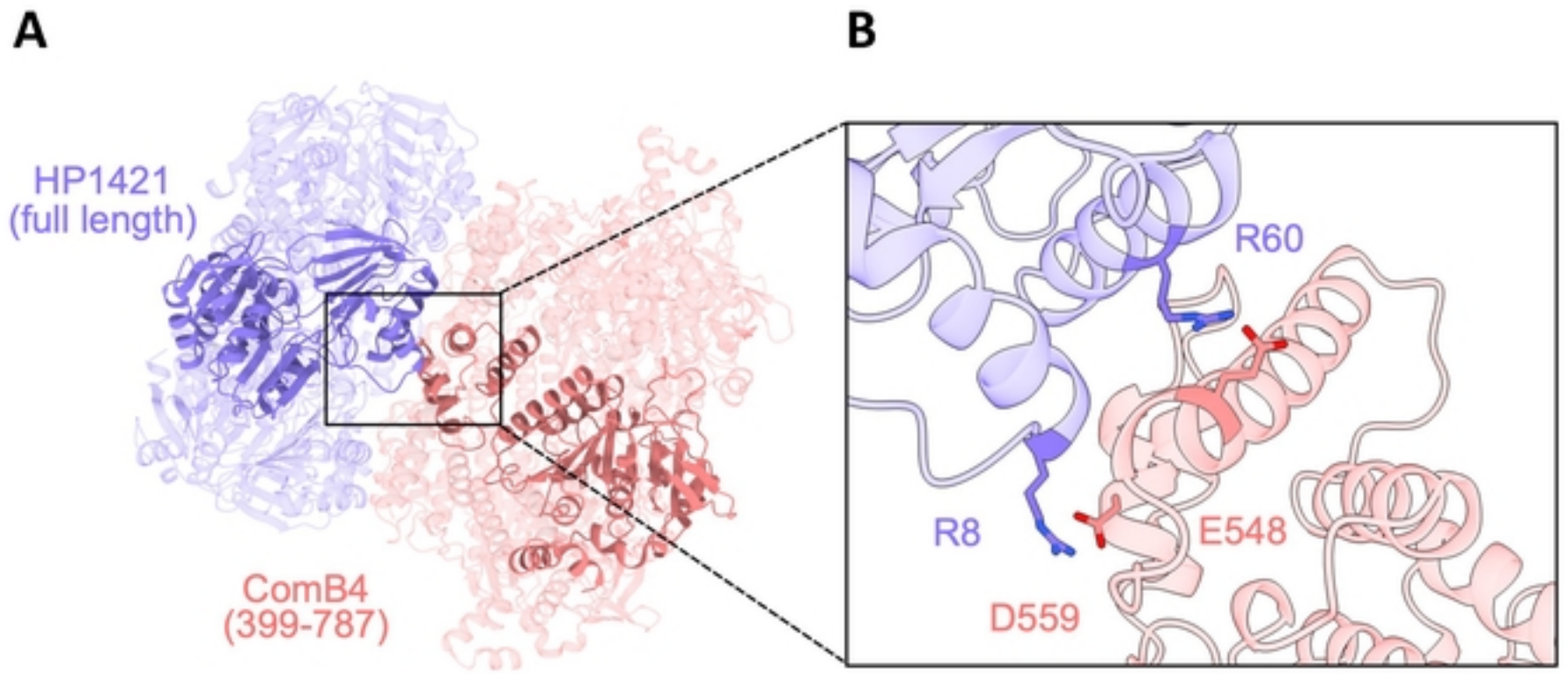

AlphaFold 3 model of the HP1421 and ComB4 double hexamer

Figure 5

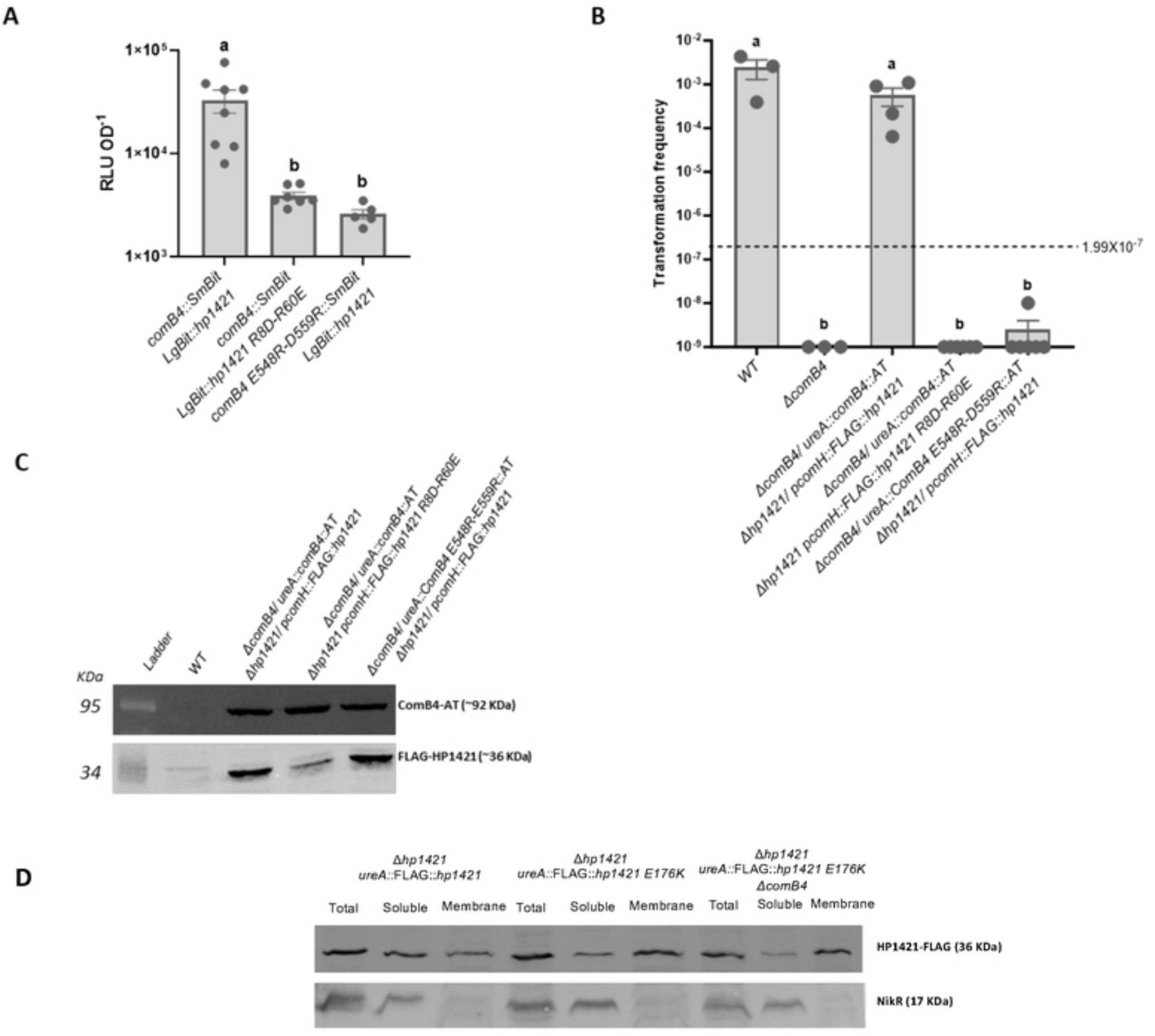
A
RLU OD-1
1×10^5
1×10^4
1×10^3
a
b
b
comB4::SmBit LgBit::hp1421
comB4::SmBit LgBit::hp1421 R8D-R60E
comB4 E548R-D559R::SmBit LgBit::hp1421
B
Transformation frequency
10^-2
10^-3
10^-4
10^-5
10^-6
10^-7
10^-8
10^-9
1.99X10^-7
a
a
b
b
b
WT
ΔcomB4
ΔcomB4/ ureA::comB4::AT Δhp1421/ pcomH::FLAG::hp1421
ΔcomB4/ ureA::comB4::AT Δhp1421 pcomH::FLAG::hp1421 R8D-R60E
ΔcomB4/ ureA::ComB4 E548R-D559R::AT Δhp1421/ pcomH::FLAG::hp1421
C
Ladder
WT
ΔcomB4/ ureA::comB4::AT Δhp1421/ pcomH::FLAG::hp1421
ΔcomB4/ ureA::comB4::AT Δhp1421 pcomH::FLAG::hp1421 R8D-R60E
ΔcomB4/ ureA::ComB4 E548R-E559R::AT Δhp1421/ pcomH::FLAG::hp1421
KDa
95
34
ComB4-AT (~92 KDa)
FLAG-HP1421 (~36 KDa)
D
Δhp1421 ureA::FLAG::hp1421
Δhp1421 ureA::FLAG::hp1421 E176K
Δhp1421 ureA::FLAG::hp1421 E176K ΔcomB4
Total
Soluble
Membrane
Total
Soluble
Membrane
Total
Soluble
Membrane
HP1421-FLAG (36 KDa)
NikR (17 KDa)

Figure 6.

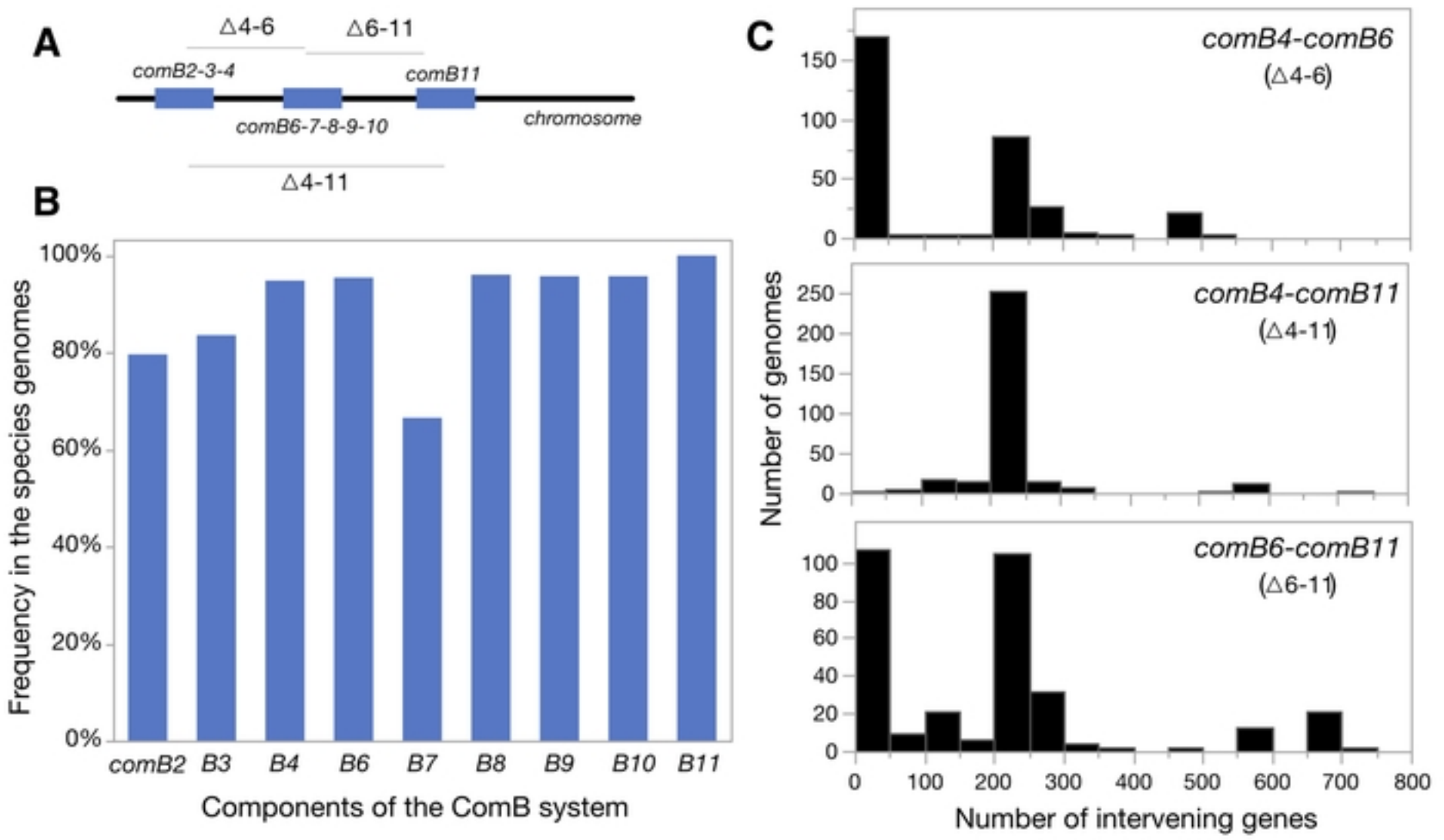
A
Δ4-6
Δ6-11
comB2-3-4
comB11
comB6-7-8-9-10
chromosome
Δ4-11
B
Frequency in the species genomes
100%
80%
60%
40%
20%
0%
comB2
B3
B4
B6
B7
B8
B9
B10
B11
Components of the ComB system
C
comB4-comB6
(Δ4-6)
comB4-comB11
(Δ4-11)
comB6-comB11
(Δ6-11)
Number of genomes
Number of intervening genes

Figure 7.

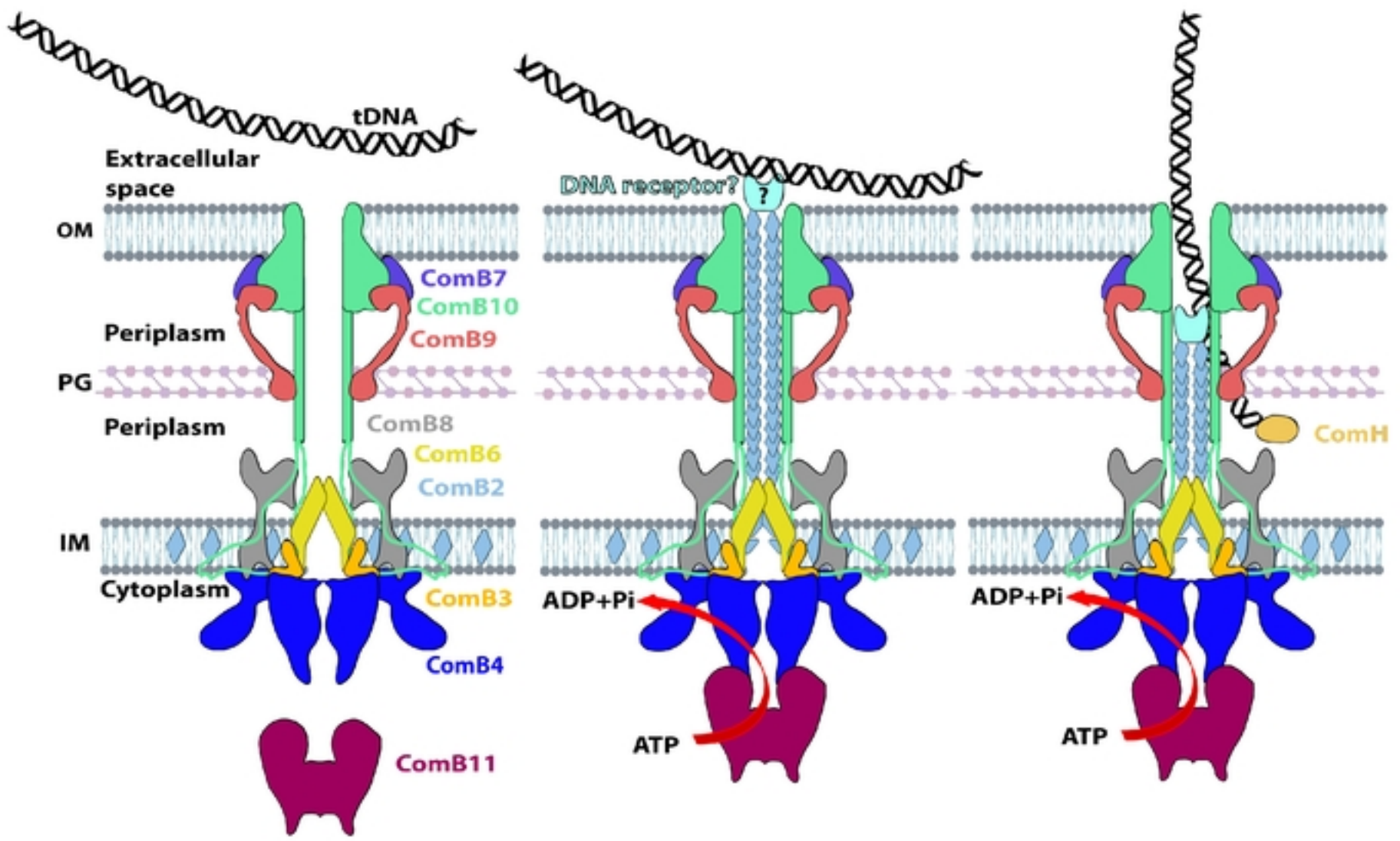
tDNA
Extracellular space
OM
ComB7
ComB10
ComB9
Periplasm
PG
Periplasm
ComB8
ComB6
ComB2
IM
Cytoplasm
ComB3
ComB4
ComB11
DNA receptor?
?
ADP+Pi
ATP
ADP+Pi
ATP
ComH

Figure 8.